Artesunate, EDTA and colistin work synergistically against MCR-negative and -positive colistin-resistant *Salmonella*

Yajun Zhai[1]†, Peiyi Liu[1]†, Xueqin Hu[1]†, Changjian Fan[1], Xiaodie Cui[1], Qibiao He[1], Dandan He[1], Xiaoyuan Ma[1], Gongzheng Hu[1*], Yajun Zhai[1*]

[1]Department of Pharmacology and Toxicology, College of Veterinary Medicine, Henan Agricultural University, Zhengzhou, Henan 450046, China

† The authors contributed equally as the first author.

[*]Corresponding authors Address: College of Veterinary Medicine, Henan Agricultural University, Zhengzhou 450002, People's Republic of China;

E-mail address: zyj90518@126.com (Yajun Zhai), yaolilab@126.com (Gongzheng Hu)

Running title: Synergy of artesunate, EDTA and colistin

Abstract

Discovering new strategies to combat the multi-drug resistance bacteria constitutes a major medical challenge of our time. Previously, artesunate (AS) has been reported to exert antibacterial enhancement activity in combination with β-lactam antibiotics, via inhibition of the efflux pump AcrB. However, combination of AS and colistin (COL) revealed weak synergistic effect against a limited number of strains, and few studies have further explored its possible mechanism of synergistic action. In this paper, we found that AS and EDTA could strikingly enhance the antibacterial effects of COL against *mcr-1*$^{-}$ and *mcr-1*$^{+}$ *Salmonella* strains either *in vitro* or *in vivo*, when used in triple combination. The excellent bacteriostatic effect was primarily related to the increased cell membrane damage, accumulation of toxic compounds and inhibition of MCR-1. The potential binding sites of AS to MCR-1 (THR283, SER284, and TYR287) were critical for its inhibition of MCR-1 activity. Additionally, we also demonstrated that the CheA of chemosensory system and virulence-related protein SpvD were critical for the bacteriostatic synergistic effects of the triple combination. Selectively targeting CheA, SpvD or MCR using the natural compound AS could be further investigated as an attractive strategy for treatment of *Salmonella* infection. Collectively, our work opens new avenues towards the potentiation of COL and revealed an alternative drug combination strategy to overcome COL resistant bacterial infections.

Keywords: artesunate/EDTA/colistin/triple combination/colistin resistant/*Salmonella*

46 **Introduction**

47 *Salmonella* is globally recognized as a major zoonotic foodborne pathogen, that responsible for food
48 poisoning, gastroenteritis and even life threatening in animals and humans (Galán-Relaño *et al*, 2023,
49 Gangathraprabhu, 2020). Antibiotics are commonly used to shorten duration of illness and reduce infectivity.
50 However, with the increasing use of antibiotics, the infections caused by multi-drug resistant (MDR)
51 pathogens, especially the carbapenemase-producing *Enterobacteriaceae*, have become the major source of
52 public-health concerns (Foletto *et al*, 2021). The shortage of new antibiotics for these MDR bacteria strains
53 has led to the re-use of polymyxins as the "last resort" antimicrobial drug with the inevitable risk of
54 emerging resistance (Falagas & Kasiakou, 2005). Colistin (polymyxin E, COL), a fatty acyl oligopeptide
55 antibiotic, is an active agent against Gram-negative (G^-) pathogens, and has been widely used to combat
56 *Salmonella* infections. Generally, COL kills bacteria through a detergent-like effect, that the polycationic ring
57 of COL electrostatically interacted with the cell envelope components, causing the competitive displacement
58 of divalent cations calcium (Ca^{2+}) and magnesium (Mg^{2+}), destabilizing the membrane, thus killing the
59 bacterium via the "self-promoted uptake" pathway (Kaye *et al*, 2016). Beyond that, other models for the
60 antibacterial activity have been reported, including vesicle-vesicle contact, hydroxyl radical death, inhibition
61 of respiratory enzymes and anti-endotoxin COL activity pathways (El-Sayed Ahmed *et al*, 2020). Until now,
62 numerous chromosomally- or plasmid-mediated mechanisms underlying polymyxins resistance in G^- bacteria
63 have been identified, including intrinsic, mutation (eg. PmrAB, PhoPQ or AcrAB-TolC mutants), adaptation
64 mechanisms or horizontally acquired resistance via the phosphoethanolamine (pEtN) transferase genes *mcr-1*
65 to *9* (Carroll *et al*, 2019; Lima *et al*, 2018; Poirel *et al*, 2017).

66 To tackle the increasing emergence of MDR pathogens, many alternative therapies, less costly and

time-consuming than drug discovery, have been new areas of current research interest, involving the combination therapy of existing agents, the drug discovery from natural products, and the evaluation of drug resistance reversers (Rosenthal, 2003). A variety of antibiotic adjuvants that may or may not have direct antibacterial effects have been widely investigated to increase the effectiveness of current antibiotics or delay the emergence of drug resistance, such as β-lactamase inhibitors, aminoglycoside-modifying enzyme inhibitors, membrane permeabilisers, and efflux pump inhibitors (Laws *et al*, 2019). Several promising inhibitors, for example zidebactam and pyrazolopyrimidine compounds have been described as the β-lactam and aminoglycoside enhancers against G^- bacteria (Moya *et al*, 2017; Stogios *et al*, 2013). Alternatively, numerous synthetic antimicrobial peptides and plant-derived natural products have been shown to possess membrane permeabilising or efflux pump inhibitory activity, with the combination of azithromycin, ciprofloxacin, imipenem *et al* (Aron & Opperman, 2016; Lin *et al*, 2015; Su & Wang, 2018).

Artesunate (AS) is a semi-synthetic derivative of anti-malarial compound artemisinin that extracted from the traditional Chinese herb Artemisia annua. Beyond remarkable antimalarial action, AS and other artemisinin derivatives, eg. dihydroartemisinin (DHA), have been proven to restored the antibacterial effect of COL against *Escherichia coli* (*E. coli*), while themselves didn't exhibited intrinsic antimicrobial activity against clinical *E. coli* isolates as well as ATCC 25922 (Wei *et al*, 2020; Zhou *et al*, 2022). In addition, AS has also been proved to enhance the effectiveness of various β-lactam and fluoroquinolones antibiotics against MDR *E. coli* via inhibiting the efflux pump AcrAB-TolC (Pan *et al*, 2020; Wei *et al*, 2020). Nonetheless, the synergistic effect between AS and COL were only observed in a limited number of strains, with a modest reversal effect. Therefore, few studies have been undertaken to evaluate its underlying mechanism. Under this circumstance, it is meaningful to explore new drug combinations between AS and COL against MDR bacteria.

88 Encouragingly, in this study, we confirmed the prominent synergistic effects of AS and EDTA to restore the
89 antimicrobial activity of COL and its possible molecular mechanism.
90

91 ## Results

92 **Artesunate and EDTA could enhance the effects of colistin against *Salmonella* strains**

93 The antimicrobial activities of AS, EDTA or COL alone were initially investigated to the COL-sensitive
94 strains of *Salmonella* (JS, S34), COL-resistant clinical strains of *Salmonella* (S16, S20, S13, and S30), *E. coli*
95 (E16), and intrinsically COL-resistant species (*Morganella morganii* strain M15, *Proteus mirabilis* strain P01).
96 Results showed that AS or EDTA alone had no direct antibacterial activity against these strains, with the
97 minimum inhibitory concentrations (MICs) 1250 or > 125 mg/L (Table supplement 1). Excepting for the two
98 intrinsically COL-resistant strains M15 and P01, there were only slight decrease of COL MICs for other
99 strains (fold changes ranging from 0 to 133), when the sub-inhibitory concentrations (1/4, 1/8, 1/16 MIC) of
100 AS or EDTA were combined with COL (namely AC or EC) (Table supplement 1). Whease, we found marked
101 decrease of COL MICs (up to 60000 fold), after three drug combinations (namely AEC) (Table 1). These
102 results indicated that when used simultaneously with COL, AS and EDTA exerted antibacterial enhancement
103 activity for *Salmonella* and *E. coli*, but not the intrinsically COL-resistant species. Thus, AS and EDTA could
104 be considered as adjuvants to reverse COL resistance in *Salmonella*.

105 To verify the antibacterial enhancement activity of AS and EDTA, the growth curves of *Salmonella* JS,
106 S16 (*mcr-1*$^{-}$), and S30 (*mcr-1*$^{+}$) for the combined treatments were generated within 24 h (Figure 1). Generally,
107 the higher concentration of COL (2 mg/L), either alone or in combinations, was found more effective against
108 these strains than that of the lower concentration (0.1 mg/L). Compared with the control groups, when these

109 bacteria were grown in the presence of COL alone (0.1 mg/L) or different drug combinations, the
110 antimicrobial activity were not significant after incubation for 24 h (Figure 1a, b, c). By contrast, higher
111 concentration of COL (2mg/L), alone or in combinations, showed better antibacterial activity, and a gradual
112 increase in antibacterial activity was observed: AEC > AC > EC > C (Figure 1d, e, f). It's worth noting that the
113 effect of different combinations against *mcr-1*$^{+}$ strain S30 was weaker than that of *mcr-1*$^{-}$ S16 and standard
114 sensitive strain JS.
115

116 **Artesunate and EDTA enhanced the membrane-damaging effect of colistin on *Salmonella***

117 In order to gain insight into the membrane-damaging bactericidal mechanism of COL alone or combinations,
118 the damages to the bacterial outer and inner membrane (OM and IM) were severally monitored by measuring
119 the fluorescent intensity of *Salmonella* strains S16 and S30 mixed with NPN and PI. Overall, the fluorescence
120 signals of NPN and PI increased progressively with increases in the concentration of COL. After the treatment
121 of AEC, S16 and S30 both showed strongest fluorescence signals of NPN, compared to those of other groups
122 (Figure 2a, b). Nevertheless, AS treatment group also exerted a significant increase of fluorescent signal,
123 although it is not as strong as that of AEC treated group. Meanwhile, there were rapid and significant increase
124 in fluorescence of PI, when AEC or EC were added to bacterial cultures, and the two regimens played
125 dominant roles in low or high concentrations of COL, respectively (Figure 2c, d). Therefore, these results
126 indicated that the bacterial cell surfaces were severely damaged after the AEC treatment, via the rapid
127 perturbations of OM and IM. Subsequently, the morphological changes of *Salmonella* strain S16 treated with
128 different regimens were further investigated using Scanning electron microscope (SME) analysis to confirm
129 the above membrane-damaging effect. As shown in Figure 3, SEM micro-graphs of control and solvent treated

130 groups revealed that cells were short and rod-shaped, with rounded ends and intact cell membranes. As
131 expected, after exposure to COL alone and different regimens, noticeable damage to the OM were observed,
132 especially in AC and AEC treated group. Exposure to AC and AEC leading to cell damages characterized by
133 folds, crevices, and depressions, which further suggested that AS and EDTA combined with COL resulted in
134 remarkable bacterial membrane injury for antibacterial activity. Collectively, these data confirmed the
135 membrane-damaging effects of AS, EDTA and COL combination against *Salmonella*.
136
137 **AEC combination could collapse the Δψ component of Proton Motive Force (PMF) in *Salmonella***
138 In bacteria, the PMF, alternatively known as electrochemical proton gradient, is result from the extrusion of
139 protons by the electron transport chain, and made up of the sum of two parameters: an electric potential (Δψ)
140 and an osmotic component (ΔpH) (Farha *et al*, 2013). It has been reported to drives vital cellular processes in
141 bacteria, including ATP synthesis, antibiotic transport, and cell division (Le *et al*, 2021). Therefore, PMF
142 dissipation was considered as a promising strategy for combating microbial pathogens. In this work, we
143 explored whether the antibacterial synergism activities of different combinations were accompanied by
144 dissipation of PMF in cells. We uncovered that when compared to that of other groups, AEC treatment caused
145 a rapid collapse of Δψ component, as shown by the increase in fluorescence values of $DISC_3(5)$ (Figure 2e, f).
146 But none of these combinations observed significant dissipation of ΔPH, when compared to that of control
147 group (Figure 2g, h). The above results indicated that AEC treatment was able to dissipate selectively the Δψ
148 component of PMF.
149
150 **Other reactive oxygen species (ROS), not H_2O_2, contributed to the AS and EDTA-mediated efficacy**

151 **enhancement of COL**

152 ROS including superoxide (O^{2-}), hydrogen peroxide (H_2O_2), and hydroxyl radical ($\cdot$OH), are commonly
153 generated during the electron transfer process, which has been considered to associated with the lethal action
154 of diverse antimicrobials. Subsequently, we investigated whether the addition of AS and EDTA could facilitate
155 the intracellular ROS generation and stimulate the ROS-mediated killing. As shown in Figure 2i, j, compared
156 to control group, total ROS increases in S16 and S30 strains were observed in AC and AEC groups either after
157 0.1 or 2 mg/L COL was added, but for COL alone and EC groups, the increase were only occured after the
158 addition of a relatively high COL concentration (2 mg/L). In addition, the ROS accumulation level was further
159 increased in AEC group, when extending the incubation time period to 6 h (Figure supplement 1). Moreover,
160 we found that H_2O_2 did not contribute to the increase of total ROS, as there was no significant difference in
161 intracellular level of H_2O_2 among all the groups Figure 2k, l. Collectively, these observations supported a role
162 for ROS in AS and EDTA-mediated efficacy enhancement of COL.

163

164 **The transcriptome data exhibited more robust changes than that of metabolome among different**
165 **comparison groups.**

166 A total of 6944 differentially expressed genes (DEGs) were performed KEGG pathway enrichment analysis,
167 of which 1832 and 5112 transcripts were included in S16 and S30 strains, respectively (Figure supplement 2).
168 Several canonical pathways, including two-component system (TCS), flagellar assembly and ABC
169 transporters pathways, indicating similar directional changes in both strains were selected for further analysis,
170 as shown in Figure 4. Since AEC incubation has displayed excellent antibacterial effects, we expected to
171 screen the significantly differentially expressed genes (SDEGs) with similar variations in AEC vs. C, AEC vs.

172 AC, and AEC vs. EC groups, and the SDEGs involved in TCS (*pagC*, *cheA*, *ompF*, *et al.*), flagellar assembly

173 (*flgK*, *flgL*, *fliD*, *et al*) and ABC transporters (*oppuBB*, *osmX*, *gltI*, *dppA*, *et al.*) were selected (mostly

174 down-regulated) and summarized in Figure 5.

175 Unlike transcriptome changes, the metabolite alterations were much less abundant among AEC vs. C,

176 AEC vs. AC, and AEC vs. EC groups, either in S16 or S30 strain. Unluckily, we demonstrated that there were

177 low correlation between the metabolome and transcriptome data. According to the enrichment analysis,

178 archidonic acid metabolism (down-regulated), degradation of aromatic compounds (up-regulated), taurine and

179 hypotaurine metabolism (up-regulated) were the most prominent pathways showing differences primarily in

180 AEC vs. C group (Figure 6).

181

182 **AS+EDTA+COL combination therapy is a promising therapeutic against *Salmonella* infection *in vivo***

183 The excellent bactericidal synergism against *Salmonella in vitro* of AEC combination further prompted us to

184 confirm the effect *in vivo* for *Salmonella* S30 (*mcr-1*$^{+}$) infected mouse models. Consistent with the synergistic

185 bactericidal activity of AS, EDTA, and COL, the combination of AC (7.13 $\log_{10}$CFU/g Liver, 6.91 $\log_{10}$CFU/g

186 spleen), EC (7.33 $\log_{10}$CFU/g Liver, 6.88 $\log_{10}$CFU/g spleen), and AEC (6.51 $\log_{10}$CFU/g Liver, 6.52

187 $\log_{10}$CFU/g spleen) outperformed single-drug treatments of COL (7.44 $\log_{10}$CFU/g Liver, 7.05 $\log_{10}$CFU/g

188 spleen) and AS (7.54 $\log_{10}$CFU/g Liver, 7.02 $\log_{10}$CFU/g spleen). In particular, in the AEC combination

189 treated samples, there were far fewer bacteria burden in spleen and liver when compared to other groups

190 (Figure 7). These disparity *in vivo* further illustrate the synergy of AS and EDTA in combination with COL.

191

192 **Discussion**

193 **Membrane-damaging played a crucial role in the synergistic antimicrobial effects of AS+EDTA+COL**

194 **combination**

195 COL is an increasingly important antibiotic against serious infections caused by G^- bacteria. It damages both

196 the OM and IM layers of the cell surface by targeting LPS, displacing cations that form bridges between LPS

197 molecules, and thereby leading to disruption of the cell envelope and bacterial lysis (Sabnis *et al*, 2021). Our

198 data showed that the AEC combination could permit ingress of NPN fluorophore into the OM, as well as the

199 membrane impermeant dye PI into the IM, which fluoresces upon contact with DNA in the bacterial

200 cytoplasm (Figure 2a-d). Thus, it indicated AEC combination has punched holes in both the OM and IM of

201 whole bacterial cells. The considerably deformed of cell membranes observed by SEM further supported the

202 above results that the membrane integrity, and permeability were damaged after AEC incubation. Considering

203 that EDTA is used as a complexing agent, we tried to explore if it could assist COL to destroy the bacterial

204 membrane and reduce their survival by chelating cations that stabilize LPS and the outer membrane.

205 Nevertheless, we found minimal changes in MICs of different combinations to S16 and S30 strains, after

206 different cations (Na^+, K^+, Ca^{2+}, Mg^{2+}, Mn^{2+}, Zn^{2+}) were supplemented (Table supplement 2). In contrast, LPS

207 treatment resulted in dose-dependent changes in MICs of different combinations to S16 and S30 strains (Table

208 supplement 3), which indicated that LPS on cell membrane was a crucial target for AEC to injure cell

209 membrane and exert prominent antibacterial effects.

210 Whilst it is commonly believed that COL acts against G^- bacteria by cell membrane lysis, we

211 hypothesised that alterations in bacterial membrane lipid composition may also be a possible Achilles' heel to

212 increase efficacy of COL after the AEC incubation in this paper. The metabolomic results of AEC vs. C group

213 in this study showed a significant decrease of prostaglandins (PGs) in arachdonic acid metabolism pathway

214 (Figure 6). Arachidonic acid is a highly abundant long chain polyunsaturated fatty acid in vertebrates, which
215 have been proposed to have antibacterial roles. Exogenous Arachidonic acid has been reported to readily
216 incorporated into the synthesis pathways of membrane phospholipids, and exert detrimental effects on
217 membrane integrity by perturbing membrane ordering, altering membrane composition and increasing fluidity
218 (Eijkelkamp *et al*, 2018; MacDermott-Opeskin *et al*, 2022). PGs are lipid compounds derived from
219 arachidonic acid, which has been demonstrate to enhance biofilm development and fungal load in the murine
220 vaginae of *Candida albicans* (Ells *et al*, 2011). Therefore, we speculated that the down-regulated lipid
221 compounds PGs may lead to perturbtion of membrane phospholipids in cell membranes and reduce microbial
222 viability.

223 Accumulation of toxic compounds may also be held responsible for the membrane damage. We noted
224 that there were significant accumulation of styrene in both S16 and S30 strains (Figure 6). Styrene is naturally
225 present as a minor metabolite, that can be synthesized at low levels by several microorganisms, like
226 *Pencillium camemberti* and members of the *Styracaceae* family (Yeh *et al*, 2022). However, styrene itself is
227 toxic to most cell types, and its hydrophobic molecules could readily partition into bacterial membrane,
228 resulting in membrane disruption and cell death (Lian *et al*, 2016). Additionally, we found that the taurocholic
229 acid and protocatechuic acid were up-regulated respectively in S16 and S30 strains (Figure 6). Taurocholic
230 acid is usually a major component of the selective culture medium, for example MacConkey agar, for G^-
231 bacteria, which has also been confirmed as a secondary metabolite of marine isolates and the soil bacterium
232 *Streptococcus faecium*. Sannasiddappa *et al* have proved that taurocholic acid were able to inhibit growth of
233 *Staphylococcus aureus* through increasing membrane permeability and disruption of the PMF (Sannasiddappa
234 *et al*, 2017). Protocatechuic acid has been demonstrated to exert antimicrobial effects by disrupting the cell

235 membranes, preventing bacterial adhesion and biofilm formation (Bernal-Mercado *et al*, 2018; Stojković *et al*,
236 2013). Consequently, these toxic compounds were anticipated to accelerate the destruction of cell membrane
237 and thus enhance the antibacterial activity.
238
239 **The CheA of chemosensory system and virulence-related protein SpvD were critical for the**
240 **bacteriostatic synergistic effect of AEC combination**
241 Flagellar motility is intimately connected to chemotaxis, biofilm formation, colonisation and virulence of
242 many bacterial pathogens. It is generally regulated by a chemotactic signaling system, which enables their
243 movement toward favorable conditions and invade their hosts (Bolton, 2015). The chemotaxis proteins CheA,
244 CheW, CheY, methyl-accepting chemotaxis proteins (MCPs) have already been identified as core components
245 and present in all chemotaxis systems (Minamino *et al*, 2022). The *Salmonella* flagellum is composed of about
246 30 different proteins, such as FliD (the filament cap), FlgK and FlgL (the hook-filament junction) *et al*
247 (Minamino *et al*, 2022). Tellingly, we have found an extensive down-regulation of chemotaxis and flagellar
248 assembly related genes in S16 and S30 strains after AEC incubation (Figure 5a-d). Meanwhile, the swimming
249 motility of the strains were decreased after AEC incubation (Figure supplement 5). The overexpression of
250 *cheA* in S16 strain, but not *cheY*, *STMDT2-34621*, *aer*, *fliD*, *fliT*, could lead to noticeable increases of MICs
251 by 4 to 32 fold, after EC or AEC incubation (Table supplement 4). These results suggested that the down
252 regulation of the central component of chemosensory system CheA may affect both chemotactic motility and
253 general structure of flagellum, thus attenuating *Salmonella* survival after AEC treatment.
254 In addition to the above findings, we also noted that there were relatively large number of SDEGs, most
255 of them were down-regulated, enriched in the ABC transports pathway in S16 and S30 strains after AEC

256 incubation (Figure 5e, f). ABC transporters are a class of transmembrane transporters, which mediate uptake
257 of micronutrients, including saccharides, amino acids, metal ions *et al* and have also been shown to protect
258 bacteria from hazardous compounds (Nguyen & Götz, 2016; Wang *et al*, 2023). The *opuBB* and *opuBA*
259 encode components of the ABC-type proline/glycine betaine transport system, and their up-regulation were
260 proved to promote accumulation of proline that acted as an osmoprotectant (Dupre *et al*, 2019). Similarly, the
261 OsmU osmoprotectant systems, consisting of OsmV, OsmW, OsmY, and OsmX, were identified to enable
262 bacterial survival at high-osmolarity through the accumulation of glycine betaine (Frossard *et al*, 2012). The
263 *gltI* gene encodes glutamate/aspartate transport protein, and its deletion in *E. coli* were shown to result in
264 attenuated survival under antibiotics, acid, and hyperosmotic stressors (Niu *et al*, 2023). Furthermore, the
265 dipeptide permease operon (*dpp*), especially *dppA*, has been reported as an essential enzyme for survival of
266 *Mycobacteria tuberculosis* under nutrient starvation conditions, and was associated with reduced bacterial
267 burden in chronically infected mice in knockout studies (Fernando *et al*, 2022). Nevertheless, the
268 overexpression of *opuBB*, *gltI*, *dppB* and *dppC* genes caused no detectable change in MICs for S16 strain after
269 AEC incubation (Table supplement 4). Thus, these observations suggest that overexpression of these SDEGs
270 in ABC transporters were not sufficient enough for causing changes in COL susceptibility, and additional
271 factors may be required for the excellent bactericidal activity of AEC.

272 Besides that, we also noticed that the expression levels of *Salmonella* infection related genes *sseJ*, *spvD*
273 and ribosomal protein genes *rpmJ*, *rpmE* were all strikingly changed in S16 strain (Figure supplement 4a).
274 SseL and SpvD are effectors of *Salmonella* pathogenicity islands 1 and 2 (SPI1 and SPI2), which are required
275 for full virulence during animal infections (Coombes *et al*, 2007; Grabe *et al*, 2016). The *rpmJ* gene codified a
276 part of 50S ribosomal subunit, and its up-regulation has been related to size increase and slow growth of *E.*

277 *coli* cells under starvation conditions (Peredo-Lovillo *et al*, 2019). The overexpression of *spvD* gene in S16
278 strain could attenuate the antibacterial activity of AC and AEC regimen with 4 fold increase in MICs (Table
279 supplement 4), which indicated that the virulence-related protein SpvD contributed to the increase of COL
280 susceptibility after AEC incubation.
281
282 **Artesunate can be considered as a potential MCR-1 inhibitor that enhances the efficacy of colistin**
283 During our research process, several phenomenon have caught our attention, that the synergistic effect of AEC
284 combination was irrelevant to whether the *mcr-1* gene exists or not, and the *mcr-1*$^-$ strain S16 exhibited more
285 robust changes than that of *mcr-1*$^+$ strain S30 in different KEGG pathways. These results indicated that AS
286 and EDTA were possible to exert synergistic effects by blocking the broad-spectrum resistance mechanisms
287 (eg. efflux pumps, membrane damage), and coupling with the drug-specific resistance mechanisms (eg.
288 MCR-1, β-lactamase). Previously, AS was capable of significantly enhancing the antibacterial activity of β
289 -lactam antibiotics against *E. coli*, via inhibition of the efflux pumps such as AcrB, NorA, NorB, and NorC
290 (Jiang *et al*, 2013; Li *et al*, 2011). Molecular docking experiments showed that AS could dock into AcrB very
291 well forming five hydrogen bonds with Ser46, Gln89 and Gln176 (Wu *et al*, 2013). Whereas, in this paper, the
292 inhibitory actions of different drug combinations on efflux pump were only observed in *mcr-1*$^-$ strain S16,
293 regardless of whether AS was added (Figure supplement 4c). Therefore, we hypothesised that AS may exert
294 synergistic effects with COL against *mcr-1*$^+$ S30 strain by targeting MCR-1 rather than efflux pump.
295 MCR-1 comprises two distinct domains, an N-terminal transmembrane domain and a soluble C-terminal
296 α / β / α sandwich domain where the active site located. The active site contains a concentration of
297 metal-binding residues to accommodate between one and four zinc ions (Wei *et al*, 2018). Several crystal

298 structures of the soluble domain have been well studied, and six residues GLU246, THR285, HIS395, ASP465,
299 HIS466, and HIS478 were found conserved among pEtN transferases (Ma *et al*, 2016). Especially the
300 THR285 residue, which was highly conserved and providing a distinct electronegative potential to attract and
301 bind the substrate pEtN (Son *et al*, 2019). Mutations of these residues and stripping the metals by EDTA could
302 re-establish polymyxin B antibacterial action (Hinchliffe *et al*, 2017; Hu *et al*, 2016; Stojanoski *et al*, 2016).
303 In this paper, we firstly analyzed the relative expression of *mcr-1* in S30 strain after the incubation of different
304 drug combinations, and found a striking down-regulation of *mcr-1* gene whether after AC, EC incubation or
305 AEC incubation, when compered to that of A and E treatment (Figure supplement 4b). Additionally, we
306 performed the molecular docking between AS and MCR-1 to predict if there were possible interactions, and
307 found that AS could bind to the residues arrounding the reported key residues within MCR-1 of *E. coli*,
308 forming seven hydrogen bonds with THR283, SER284, TYR287, PRO481, and ASN482 residues (Figure
309 supplement 4e). The interaction between AS and MCR-1 was further proved by competitive inhibitory assays,
310 that the binding of AS with MCR-1 was blocked after the addition of polypeptide P_u (containing unmutated
311 THR283, SER284, and TYR287 sites) and lead to significant increases of MICs by 8 fold after AC or AEC
312 treatment (Table supplement 5). Nevertheless, we also noticed that the blocking effect could not be removed
313 by peptide P_m (containing mutated THR283, SER284, and TYR287 sites) when EDTA exists. We supposed
314 that EDTA may chelate zinc ions that required for MCR-1 activity. Thus, we suggested that AS could be
315 developed as the a MCR-1 inhibitor, and coupled with the chelating agent EDTA may favor to additionally
316 magnify its inhibitory effect.
317
318 **A mixed blessing: the excellent antibacterial activity and potential toxicity of AEC combination**

319 In the preceding years, several studies have reported on the synergistic effects of COL with different
320 candidates, such as antimicrobial agents, natural compounds and synthetically prepared molecules (Cui *et al*,
321 2024, Yi *et al*, 2022). Nevertheless, the potential toxicity of these combination therapy will be the prime
322 concern affecting their clinical application, and a similar concern has also been raised for the AEC
323 combination in this study. Although *in vitro* studies have determined that with increasing dose of AS and
324 EDTA, the antibacterial synergistic activity was gradually enhanced, and meanwhie, may also resulting in
325 more toxic side effects. Thus, In our study, the 1/8 MICs of AS and EDTA were selected to ensure excellent
326 antibacterial activity whereas minimize the potential toxicity. The toxic side effects of AEC combination may
327 be most probably caused by COL, which is well known to present several adverse toxic effects, and the
328 dose-dependent nephrotoxicity is the most reported (Lu *et al*, 2016, Visentin *et al*, 2017). Conversely, EDTA
329 and AS may be low toxicity. When used in combination with COL or AB569, EDTA has been proved to
330 synergistically overcome the COL-resistant *Klebsiella pneumonieae* and MDR *Acinetobacter baumannii* with
331 the concentration of 12000 mg/L and 73 mg/L, respectively (Bari *et al*, 2023, Bogue *et al*, 2021). These
332 concentrations were reported non-toxic to primary adult human skin (dermal) fibroblasts and other normal
333 body cells, which may also apply to the lower concentrations of EDTA (15.6 mg/L) used in AEC combination
334 (Shein *et al*, 2021). Additionally, AS has been found to exert multiple pharmacological actions including
335 anti-malaria, anti-tumor, anti-viral and anti-inflammatory effects, which has displayed a relatively safe toxicity
336 profile with the LD_{50} values being 4223 mg/kg (Cheong *et al*, 2020). However, the potential toxic effects of
337 AEC combination is still unknown and requires further investigations.

338 In summary, our results established that the combination of COL with AS and EDTA was a promising
339 candidate for combating infections caused by MCR-negative and -positive COL-resistant *Salmonella*. The

340 membrane-damaging effect, accumulation of toxic compounds, inhibition of MCR-1 were supposed to play
341 synergistic roles in reversing COL resistance of *Salmonella* (Figure 8). The CheA of chemosensory system
342 and virulence-related protein SpvD were critical for the bacteriostatic synergistic effects of AEC combination.
343 Selectively targeting CheA, SpvD or MCR using the natural compound AS could be further investigated as an
344 attractive strategy for treatment of *Salmonella* infection.
345

346 ## Materials and Methods

347 **Bacteria strains and agents**

348 A total of 9 bacteria strains were used in this study (Table 1), including a multidrug-susceptible standard strain
349 of *Salmonella* Typhimurium CVCC541 (named as JS), a COL-susceptible clinical strain of *Salmonella*
350 (named as S34), four COL-resistant clinical strains of *Salmonella* (named as S16, S20, S13, and S30), a
351 COL-resistant clinical strain of *Escherichia coli* (named as E16), and two strains of intrinsically COL-resistant
352 species (*Morganella morganii* strain M15 and *Proteus mirabilis* strain P01). COL was purchased from
353 Shengxue Dacheng Pharmaceutical, China. COL and EDTA-2Na were both dispersed into water at final
354 concentration of 640 mg/L and 10000 mg/L, respectively. AS was purchased from Meilunbio (Dalian, China)
355 and dissolved in water with 10% (V/V) N, N-dimethylformamide at a final concentration of 5000 mg/L. The
356 1-N-phenylnaphthylamine (NPN) was purchased from Sigma-Aldrich, USA. Propidium iodide (PI) was
357 purchased from Thermo Fisher Scientific, USA. The 3,3-dipropylthiadicarbocyanine iodide $DiSC_3(5)$ and
358 ethidium bromide (EtBr) were purchased from Aladdin, China. BCECF-AM, Reactive Oxygen Species Assay
359 Kit, and Hydrogen Peroxide Assay Kit were purchased from Beyotime, China.
360

361 **Antibacterial activity *in vitro***

362 **1. Antimicrobial susceptibility testing.** The MICs of COL, AS, and EDTA against all strains were
363 determined by the 2-fold serial broth microdilution method according to CLSI guidelines (Wayne, 2021) The
364 double and triple combination strategies were carried out as follow: AS (1/4, 1/8, or 1/16 MIC of AS)+ COL,
365 EDTA (1/4, 1/8, or 1/16 MIC of EDTA) + COL, AS (1/4 MIC of AS)+ EDTA (1/4, 1/8, 1/16 or 1/32 MIC of
366 EDTA) + COL, AS (1/8 MIC of AS)+ EDTA (1/4, 1/8, 1/16 or 1/32 MIC of EDTA) + COL. These medication
367 strategies, including COL alone, AS + COL, EDTA + COL, AS + EDTA + COL, were abbreviated as C, AC,
368 EC, and AEC, respectively. When determining the MICs of COL after drug combinations, AS or/and EDTA
369 were pre-added into MHB broth with different final concentrations, namely 1/4, 1/8, 1/16 or 1/32 MIC of AS
370 (312.5, 156.25, 78.13, 39.06 mg/L) or EDTA (for example 31.25, 15.63, 7.81, 3.91 mg/L for JS, S16 and S30
371 strains), then COL was added and diluted to make a 2-fold dilution series. The lowest concentrations with no
372 visible growth of bacteria were defined as MIC values of COL after drug combinations.

373 **2. Time-kill assays.** Time-kill assays were performed against the *Salmonella* strains JS, S16 (*mcr-1*$^{-}$), and S30
374 (*mcr-1*$^{+}$) with COL alone as well as in combinations (AC, EC, AEC). When combined with COL (0.1 or 2
375 mg/L), AS and EDTA were added at final concentrations equivalent to their 1/8 MICs. Overnight cultures
376 were diluted 1:100 in fresh LB medium and grown to an OD_{600} of 0.5, then treated with different
377 combinations for 24 h. The cultures were serially diluted 10-fold and spreaded over sterile nutrient agar at 0.5,
378 4, 8, 12 and 24 h. Bacterial colonies on individual plates were counted after overnight incubationat 37 ℃ and
379 expressed as the $\log_{10}$ of colony forming units/mL (CFU/mL).

380

381 **Fluorescent probe-permeability assays**

382 Overnight cultures of *Salmonella* strains S16 (*mcr-1*$^-$) and S30 (*mcr-1*$^+$) were diluted 1:100 in fresh LB
383 medium and grown to an OD_{600} of 0.7. Cells were harvested and washed twice with PBS or HEPES, then
384 re-suspended in the same buffer to $OD_{600} \approx 0.5$ for further analysis. Different drug combinations or
385 Fluorescent probes were added and incubated when necessary. The medication strategies used in the
386 fluorescence probe assays were as follow: C, AC, EC, and AEC. The final concentration of COL was 0.1 or 2
387 mg/L, when used alone or in drug combinations. AS and EDTA were added at final concentrations equivalent
388 to their 1/8 MICs, when used in drug combinations. Fluorescence intensity were measured with Spark 10M
389 microplate spectrophotometer (Tecan, Switzerland).

390 **1. Cell membrane integrity assay.** Bacterial suspensions in HEPES were mixed with either fluorescent probe
391 1-N-phenylnaphthylamine (NPN) or propidium iodide (PI) to a final probe concentrations of 10 μM for NPN
392 or 15 μM for PI. After incubation at 37℃ for 0.5 h, bacterial suspensions were then mixed with different
393 drug combinations and incubated for another 1 h. Fluorescence measurements were then taken with the
394 excitation wavelength at 350 nm (or 535 nm) and emission wavelength at 420 nm (or 615 nm) for NPN (or
395 PI).

396 **2. Proton motive force assay.** Bacterial suspensions in PBS were incubated with either
397 3,3-dipropylthiadicarbocyanine iodide ($DiSC_3(5)$, 0.5 μM) or pH-sensitive fluorescent probe BCECF-AM (20
398 μM) for 0.5 h to determine the membrane potential ($\Delta\psi$) and pH gradient (ΔpH). Then these suspensions were
399 mixed with different drug combinations and incubated for another 1 h. Finally, the fluorescence were
400 measured with the excitation wavelength of 622 nm (or 488 nm) and emission wavelength of 670 nm (or 535
401 nm) for $DiSC_3(5)$ (or BCECF-AM).

402 **3. Total ROS measurement**

403 The ROS-sensitive fluorescence indicator 2', 7'-dichlorodihydro-fluorescein diacetate (DCFH-DA, 10 μM)
404 was used to assess the ROS levels in bacterial cells. Bacterial suspensions in PBS were mixed with DCFH-DA
405 and incubated for 0.5 h, then different drug combinations were added and incubated for another 1 h and 6 h.
406 Finally, fluorescence intensity were measured at an excitation wavele of 488 nm and an emission wavelength
407 of 525 nm.

408 **4. Efflux pump assay.** Bacterial suspensions in PBS were incubated with ethidium bromide (EtBr) for 0.5 h,
409 in a final concentration of 5 μM. Then different drug combinations were added and incubated for another 1 h,
410 then the accumulation of EtBr in the cells were evaluated with excitation wavelength of 530 nm and barrier
411 filter of 600 nm.

412

413 **H_2O_2 assay**

414 The bacterial culture conditions and sample preparation were same as the fluorescent probe-permeability
415 assays section. The luminescence absorbancy were measured by a Spapk 10 M Microplate reader (Tecan,
416 Switzerland). The cellular H_2O_2 levels were assessed according to the kit procedure by using an Hydrogen
417 Peroxide Assay Kit. Cells samples were prepared as described above and incubated with different drug
418 combinations for 1.5 h. Cell precipitates were collected by centrifugation (10000 rpm), and 200 μL lysis
419 solution were added under gentle shaking. Supernatants were then taken for luminescence (Abosorbance)
420 detection at 560 nm.

421

422 **Scanning electron microscope (SME)**

423 Overnight S16 (*mcr-1*$^-$) culture was diluted 1:100 in fresh LB medium and grown to an OD_{600} of 0.7. Cells
424 were then divided equally and different drug combinations were added, same as that in the fluorescent
425 probe-permeability assays section. After 6 h incubation at 37 ℃, cells were washed three times with PBS and
426 fixed with 2.5% glutaraldehyde at 4 ℃ for 24 h. Samples were then stained in 1% osmium tetroxide and
427 dehydrated in a series of increasing ethanol concentrations (30% – 100%). The processed samples were dried
428 in Critical Point Dryer (Quorum K850) and sputter-coated with gold. Finally, samples were observed and
429 images were taken with SEM (HITACHI, SU8100).
430
431 **Omics analysis**
432 Overnight cultures of S16 (*mcr-1*$^-$) and S30 (*mcr-1*$^+$) were diluted 1:100 in fresh LB medium and grown to an
433 OD_{600} of 0.5. Cells were divided equally and different drug combinations were used, including C, AC, EC, and
434 AEC. When combined with COL (2 mg/L), AS and EDTA were added at final concentrations equivalent to
435 their 1/8 MICs. Samples were continually incubated 6 h, then washed three times with PBS and fast-frozen in
436 liquid nitrogen for further use. Transcriptome and metabolome analysis were performed among different
437 comparison groups, including AC vs. C, EC vs. C, AEC vs. AC, and AEC vs. EC, and carried out by
438 Novogene Co. Ltd (Beijing, China).
439 **1. Transcriptome analysis**
440 The clean reads were mapped to the *Salmonella* Typhimurium DT2 genome (HG326213.1) from NCBI using
441 Bowtie2. The SDEGs were screened with a p value $\leq$ 0.05 and $|\log_2 \text{Fold Change}| \geq 1$. ClusterProfiler
442 software were used to analysis the Gene Ontology functional enrichment (GO, https://geneontology.org/) or
443 Kyoto Encyclopedia of Genes and Genomes pathway enrichment (KEGG,

444 https://www.kegg.jp/kegg/pathway.html) of SDEGs.

445 **2. Metabolome analysis**

446 In this study, Samples were analyzed by the non-targeted metabolomics with Liquid Chromatography-tandem
447 Mass Spectrometry (LC-MS/MS) in either positive ion or negative ion mode. Compound Discoverer 3.1
448 software (Thermo Scientific, Waltham, MA, USA) was used for identification of metabolites based on the
449 exact masses and fragmentation spectra. The significant differential metabolites (SDMs) were identified with
450 VIP $\geq$ 1.0, Fold Change $\geq$ 1.2 or Fold Change $\leq$ 0.833, p value < 0.05. SDMs were then annotated and
451 classified by KEGG Database (https://www.genome.jp/kegg/pathway.html), Human Metabolome Database
452 (HMDB, https://hmdb.ca/metabolites), and Lipidmaps Database (https://www.lipidmaps.org/).

453

454 **Antibacterial activity *in vivo***

455 **Bacterial preparation:** Overnight culture of S30 (*mcr-1*$^{+}$) was diluted 1:100 in fresh LB medium and grown
456 to an OD_{600} of 0.7. Cells were harvested and washed twice with PBS, then adjusting the concentration of
457 bacterial suspensions to 1.31×10^{6} CFU/mL for further use.

458 **Animals and treatments:** A total of 36 SPF Kunming mice (Six to eight-week-old, 18-22 g, half male and
459 half female) were purchased from the Huaxing Experimental Animal Center of Zhengzhou (Zhengzhou, China)
460 and divided into six groups (n = 6 per group): (1) PBS control group; (2) COL (10 mg/kg) group; (3) AS (15
461 mg/kg) group; (4) AS (15 mg/kg) + COL (10 mg/kg) group; (5) EDTA (50 mg/kg) + COL (10 mg/kg) group;
462 (6) AS (15 mg/kg) + EDTA (50 mg/kg)+ COL (10 mg/kg) group. Each mice was intraperitoneally injected
463 with 100 μL bacterial solution (1.31×10^{5} CFU). Treatment was initiated at 2 h post infection and continued
464 for 3 days. Treatment was administered once per day by intraperitoneal injection according to the therapeutic

465 dose mentioned above. Mices were all euthanized and spleen, liver of aseptic were collected, weighed,
466 homogenized with PBS. Then the tissue homogenates were serially diluted with PBS in an appropriate amount
467 and 100 μL of each dilution was withdrawn and uniformly spread on SS agar plates. Bacterial counts were
468 computed and presented as the mean ± SD $\log_{10}$ CFU/mL, after incubated at 37℃ for 16 to 18 h. Mice were
469 maintained in a barrier facility and guaranteed strict compliance with the regulations for the Administration of
470 Affairs Concerning Experimental Animals approved by the State Council of People's Republic of China (11–
471 14–1988).The mouse experiments were approved by the Henan Science and Technology Department (protocol
472 number SCXK 2019-0002).
473
474 **Data available**
475 Transcriptome data have been submitted to the Sequence Read Archive database (SRA,
476 https://www.ncbi.nlm.nih.gov/sra) under the BioProject accession number PRJNA1036120 (S16 strain) and
477 PRJNA1036408 (S30 strain). Metabolome data have been submitted to the MetaboLights database
478 (https://www.ebi.ac.uk/metabolights) under accession number MTBLS8875. These accession numbers have
479 been released.
480
481 **Statistical analysis**
482 Statistical analysis was conducted using Graphpad prism 9 and SPSS software. All data were derived from n
483 ≥ 3 biological replicates and presented as mean ± SD. Without specific indication, differences between the
484 independent groups (* $p < 0.001$) were assessed with student's *t*-test or one-way ANOVA.
485

486 ## Supplement materials

487 **Figure supplement 1.** Intracellular accumulation of ROS in S16 and S30 strains after 6 h treatment.

488 **Figure supplement 2.** The number of DEGs are identified in S16 and S30 strains among different
489 comparison groups.

490 **Figure supplement 3.** KEGG pathway analysis of SDEGs in S16 (a, b) and S30 (c, d) strains within the
491 AC .vs. C, and EC .vs. C groups.

492 **Figure supplement 4.** (a) The SDEGs detected in *Salmonella* infection and ribosome pathways; (b)
493 Expression level of *mcr-1*; (c, d) efflux pump activity in S16 or S30 strain; (e) Putative pattern of interaction
494 between AS and MCR-1 protein.

495 **Figure supplement 5.** AS, EDTA, and COL inhibited the swimming motility of S16 (a) and S30 (b)
496 strains.

497 **Table supplement 1.** The antibacterial activities of COL, AS and EDTA against the tested strains after
498 single and double combinations

499 **Table supplement 2.** MIC values of COL against S16 and S30 strains after addition of exogenous
500 cations

501 **Table supplement 3.** MIC values of COL against S16 and S30 strains after addition of exogenous LPS

502 **Table supplement 4.** MIC values of COL against S16 strain after the overexpression of different genes

503 **Table supplement 5.** MIC values of COL against S30 strain after the incubation of polypeptides

504 **Table supplement 6.** Sequences of primers used in this study

505 **Table supplement 7.** The antibacterial activities of COL, AS and EDTA against the tested strains after
506 single and double combinations

507 **Table supplement 8.** The antibacterial activities of COL against the tested strains after single and triple
508 combinations

509 **Table supplement 9.** The MICs of different antimicrobial drugs against the S16 and S30

510 **Supplement materials and methods**

511

512 Acknowledgements

513 This work was supported by the National Natural Science Foundation of China (No. 32102716 and
514 32373069).

515 Ethical statement: This study was carried out in accordance with the guidelines of Henan Agricultural
516 University Animal Ethics Committee.

517

518 Author contributions

519 YZ and GH conceived the study. PL, XH, and CF performed experiments, results analysis and wrote the
520 original draft. XC and QH analyzed the results and wrote the original draft. DH and XM analyzed the results.
521 YZ, PL, and GH approved the final version of the manuscript.

522

523 Disclosure and competing interests statement

524 The authors declare that they have no conflict of interest.

525

526 Data Availability

527 Data have been made available freely online.

528

529 **References**

530 Aron Z and Opperman TJ (2016) Optimization of a novel series of pyranopyridine RND efflux pump
531 inhibitors. *Curr Opin Microbiol* 33: 1-6.

532 Bari AK, Belalekar TS, Poojary A and Rohra S (2023) Combination drug strategies for biofilm eradication
533 using synthetic and natural agents in KAPE pathogens. *Front Cell Infect Microbiol* 13: 1155699.

534 Bogue AL, Panmanee W, McDaniel CT, Mortensen JE, Kamau E, Actis LA, Johannigman JA, Schurr MJ,
535 Satish L and Kotagiri N (2021) AB569, a non-toxic combination of acidified nitrite and EDTA, is effective
536 at killing the notorious Iraq/Afghanistan combat wound pathogens, multi-drug resistant *Acinetobacter*
537 *baumannii* and *Acinetobacter spp. PLoS One* 16: e0247513.

538 Bernal-Mercado AT, Vazquez-Armenta FJ, Tapia-Rodriguez MR, Islas-Osuna MA and Mata-Haro V (2018).
539 Comparison of single and combined use of catechin, protocatechuic, and vanillic acids as antioxidant and
540 antibacterial agents against uropathogenic *Escherichia Coli* at planktonic and biofilm levels. *Molecules*
541 23:2813.

542 Bolton DJ (2015). *Campylobacter* virulence and survival factors. *Food Microbiol* 48: 99-108.

543 Cui X, Liu X, Ma X, Li S, Zhang J, Han R, Yi K, Liu J, Pan Y, He D, Hu G, Zhai Y (2024) Restoring colistin
544 sensitivity in colistin-resistant *Salmonella* and *Escherichia coli*: combinatorial use of berberine and EDTA
545 with colistin. *mSphere* 9: e0018224.

546 Cheong DHJ, Tan DWS, Wong FWS and Tran T (2020) Anti-malarial drug, artemisinin and its derivatives for
547 the treatment of respiratory diseases. *Pharmacol Res* 158: 104901.

548 Carroll LM, Gaballa A, Guldimann C, Sullivan G, Henderson LO and Wiedmann M (2019) Identification of
549 novel mobilized colistin resistance gene *mcr-9* in a multidrug-resistant, colistin-susceptible *Salmonella*
550 *enterica* Serotype Typhimurium isolate. *mBio* 10: e00853-19.
551 Coombes BK, Lowden MJ, Bishop JL, Wickham ME, Brown NF, Duong N, Osborne S, Gal-Mor O and
552 Finlay BB (2007) SseL is a *Salmonella*-specific translocated effector integrated into the SsrB-controlled
553 *Salmonella* pathogenicity island 2 type III secretion system. *Infect Immun* 75: 574-580.
554 Dupre JM, Johnson WL, Ulanov AV, Li Z, Wilkinson BJ and Gustafson JE (2019) Transcriptional profiling
555 and metabolomic analysis of *Staphylococcus aureus* grown on autoclaved chicken breast. *Food Microbiol*
556 82: 46-52.
557 Eijkelkamp BA, Begg SL, Pederick VG, Trapetti C, Gregory MK, Whittall JJ, Paton JC and McDevitt CA
558 (2018) Arachidonic acid stress impacts pneumococcal fatty acid homeostasis. *Front Microbiol* 9: 813
559 El-Sayed Ahmed MAE, Zhong LL and Shen C (2020) Colistin and its role in the Era of antibiotic resistance:
560 an extended review (2000-2019). *Emerg Microbes Infect* 9: 868-885.
561 Ells R, Kock JL, Albertyn J, Kemp G and Pohl CH (2011) Effect of inhibitors of arachidonic acid metabolism
562 on prostaglandin E_2 production by *Candida albicans* and *Candida dubliniensis* biofilms. *Med Microbiol*
563 *Immunol* 200: 23-28.
564 Foletto VS, da Rosa TF, Serafin MB, Bottega A and Hörner R (2021) Repositioning of non-antibiotic drugs as
565 an alternative to microbial resistance: a systematic review. *Int J Antimicrob Agents* 58: 106380.
566 Falagas ME and Kasiakou SK (2005) Colistin: the revival of polymyxins for the management of
567 multidrug-resistant gram-negative bacterial infections. *Clin Infect Dis* 40: 1333-1341.

568 Farha MA, Verschoor CP, Bowdish D and Brown ED (2013) Collapsing the proton motive force to identify
569 synergistic combinations against *Staphylococcus aureus*. *Chem Biol* 20: 1168-1178.
570 Fernando DM, Gee CT, Griffith EC, Meyer CJ, Wilt LA, Tangallapally R, Wallace MJ, Miller DJ and Lee RE
571 (2022) Biophysical analysis of the *Mycobacteria tuberculosis* peptide binding protein DppA reveals a
572 stringent peptide binding pocket. *Tuberculosis (Edinb)* 132: 102157.
573 Frossard SM, Khan AA, Warrick EC, Gately JM, Hanson AD, Oldham ML, Sanders DA and Csonka LN
574 (2012) Identification of a third osmoprotectant transport system, the OsmU system, in *Salmonella enterica*.
575 *J Bacteriol* 194: 3861-3871.
576 Galán-Relaño Á and Valero Díaz A (2023) *Salmonella* and Salmonellosis: An Update on Public Health
577 Implications and Control Strategies. *Animals (Basel)* 13: 3666.
578 Gangathraprabhu B, Kannan S, Santhanam G, Suryadevara N and Maruthamuthu M (2020) A review on the
579 origin of multidrug-resistant *Salmonella* and perspective of tailored *phoP* gene towards avirulence. *Microb*
580 *Pathog* 147: 104352.
581 Grabe GJ, Zhang Y, Przydacz M, Rolhion N, Yang Y, Pruneda JN, Komander D, Holden DW and Hare SA
582 (2016) The *Salmonella* effector SpvD is a cysteine hydrolase with a serovar-specific polymorphism
583 influencing catalytic activity, suppression of immune responses, and bacterial virulence. *J Biol Chem* 291:
584 25853-25863.
585 Hinchliffe P, Yang QE, Portal E, Young T, Li H, Tooke CL, Carvalho MJ, Paterson NG, Brem J, Niumsup PR
586 *et al* (2017) Insights into the mechanistic basis of plasmid-mediated colistin resistance from crystal
587 structures of the catalytic domain of MCR-1. *Sci Rep* 7: 39392.

588 Hu M, Guo J, Cheng Q, Yang Z, Chan EWC, Chen S and Hao Q (2016) Crystal structure of *Escherichia coli*
589 originated MCR-1, a phosphoethanolamine transferase for colistin resistance. *Sci Rep* 6: 38793.
590 Jiang W, Li B, Zheng X, Liu X, Pan X, Qing R, Cen Y, Zheng J and Zhou H (2013) Artesunate has its
591 enhancement on antibacterial activity of β-lactams via increasing the antibiotic accumulation within
592 methicillin-resistant *Staphylococcus aureus* (MRSA). *J Antibiot (Tokyo)* 66: 339-345.
593 Kaye KS, Pogue JM, Tran TB, Nation RL and Li J (2016) Agents of last resort: polymyxin resistance. *Infect*
594 *Dis Clin North Am* 30: 391-414.
595 Laws M, Shaaban A and Rahman KM (2019) Antibiotic resistance breakers: current approaches and future
596 directions. *FEMS Microbiol Rev* 43: 490-516.
597 Le D, Krasnopeeva E, Sinjab F, Pilizota T and Kim M (2021) Active efflux leads to heterogeneous dissipation
598 of proton motive force by protonophores in bacteria. *mBio* 12: e0067621.
599 Li B, Yao Q, Pan XC, Wang N, Zhang R, Li J, Ding G, Liu X, Wu C, Ran D *et al* (2011) Artesunate enhances
600 the antibacterial effect of β-lactam antibiotics against *Escherichia coli* by increasing antibiotic
601 accumulation via inhibition of the multidrug efflux pump system AcrAB-TolC. *J Antimicrob Chemother*
602 66: 769-777.
603 Lian J, McKenna R, Rover MR, Nielsen DR, Wen Z and Jarboe LR (2016) Production of biorenewable
604 styrene: utilization of biomass-derived sugars and insights into toxicity. *J Ind Microbiol Biotechnol* 43:
605 595-604.
606 Lu X, Chan T, Xu C, Zhu L, Zhou QT, Roberts KD, Chan HK, Li J and Zhou F (2016) Human oligopeptide
607 transporter 2 (PEPT2) mediates cellular uptake of polymyxins. *J Antimicrob Chemother* 71: 403-412.

608 Lima WG, Alves MC, Cruz WS and Paiva MC (2018) Chromosomally encoded and plasmid-mediated
609 polymyxins resistance in *Acinetobacter baumannii*: a huge public health threat. *Eur J Clin Microbiol*
610 *Infect Dis* 37: 1009-1019.
611 Lin L, Nonejuie P, Munguia J, Hollands A, Olson J, Dam Q, Kumaraswamy M, Rivera H, Jr., Corriden R,
612 Rohde M *et al* (2015) Azithromycin synergizes with cationic antimicrobial peptides to exert bactericidal
613 and therapeutic activity against highly multidrug-resistant Gram-Negative bacterial pathogens.
614 *EBioMedicine* 2: 690-698.
615 Ma G, Zhu Y, Yu Z, Ahmad A and Zhang H (2016) High resolution crystal structure of the catalytic domain of
616 MCR-1. *Sci Rep* 6: 39540.
617 MacDermott-Opeskin HI, Panizza A, Eijkelkamp BA and O'Mara ML (2022) Dynamics of the *Acinetobacter*
618 *baumannii* inner membrane under exogenous polyunsaturated fatty acid stress. *Biochim Biophys Acta*
619 *Biomembr* 1864: 183908.
620 Minamino T, Kinoshita M and Namba K (2022) Insight into distinct functional roles of the flagellar ATPase
621 complex for flagellar assembly in *Salmonella*. *Front Microbiol* 13: 864178.
622 Moya B, Barcelo IM, Bhagwat S, Patel M, Bou G, Papp-Wallace KM, Bonomo RA and Oliver A (2017) WCK
623 5107 (Zidebactam) and WCK 5153 are novel inhibitors of PBP2 showing potent "β-Lactam Enhancer"
624 activity against *Pseudomonas aeruginosa*, including multidrug-resistant metallo-β-lactamase-producing
625 high-risk clones. *Antimicrob Agents Chemother* 61: e02529-16.
626 Nguyen MT and Götz F (2016) Lipoproteins of Gram-Positive bacteria: key players in the immune response
627 and virulence. *Microbiol Mol Biol Rev* 80: 891-903.

628 Niu H, Li T, Du Y, Lv Z, Cao Q and Zhang Y (2023) Glutamate transporters GltS, GltP and GltI are involved
629 in *Escherichia coli* tolerance in vitro and pathogenicity in mouse urinary tract infections. *Microorganisms*
630 11: 1173.
631 Pan X, Cen Y, Kuang M, Li B, Qin R and Zhou H (2020) Artesunate interrupts the self-transcriptional
632 activation of MarA to inhibit RND family pumps of *Escherichia coli*. *Int J Med Microbiol* 310: 151465.
633 Peredo-Lovillo A, Dorantes-Alvarez L, Hernández-Sánchez H, Ribas-Aparicio R, Cauich-Sánchez P and
634 Aparicio-Ozores G (2019) Functional properties and microstructure of *Leuconostoc citreum* and
635 *Lactobacillus casei* shirota exposed to habanero pepper extract and inhibition of *Staphylococcus aureus*.
636 *Revista Mexicana de Ingeniería Química* 18: 115-129.
637 Poirel L, Jayol A and Nordmann P (2017) Polymyxins: Antibacterial activity, susceptibility testing, and
638 resistance mechanisms encoded by plasmids or chromosomes. *Clin Microbiol Rev* 30: 557-596.
639 Rosenthal PJ (2003) Antimalarial drug discovery: old and new approaches. *J Exp Biol* 206: 3735-3744
640 Sabnis A, Hagart KL, Klöckner A, Becce M, Evans LE and Furniss RCD (2021) Colistin kills bacteria by
641 targeting lipopolysaccharide in the cytoplasmic membrane. *eLife* 10: e65836.
642 Sannasiddappa TH, Lund PA and Clarke SR (2017) *In vitro* antibacterial activity of unconjugated and
643 conjugated bile salts on *Staphylococcus aureus*. *Front Microbiol* 8: 1581.
644 Son SJ, Huang R, Squire CJ and Leung IKH (2019) MCR-1: a promising target for structure-based design of
645 inhibitors to tackle polymyxin resistance. *Drug Discov Today* 24: 206-216.
646 Stogios PJ, Spanogiannopoulos P, Evdokimova E, Egorova O, Shakya T, Todorovic N, Capretta A, Wright GD
647 and Savchenko A (2013) Structure-guided optimization of protein kinase inhibitors reverses
648 aminoglycoside antibiotic resistance. *Biochem J* 454: 191-200.

649 Stojanoski V, Sankaran B, Prasad BV, Poirel L, Nordmann P and Palzkill T (2016) Structure of the catalytic
650 domain of the colistin resistance enzyme MCR-1. *BMC biology* 14: 81.
651 Stojković DS, Zivković J, Soković M, Glamočlija J, Ferreira IC, Janković T and Maksimović Z (2013)
652 Antibacterial activity of *Veronica montana* L. extract and of protocatechuic acid incorporated in a food
653 system. *Food Chem Toxicol* 55: 209-213.
654 Su F and Wang J (2018) Berberine inhibits the MexXY-OprM efflux pump to reverse imipenem resistance in a
655 clinical carbapenem-resistant *Pseudomonas aeruginosa* isolate in a planktonic state. *Exp Ther Med* 15:
656 467-472.
657 Shein AMS, Wannigama DL, Higgins PG, Hurst C, Abe S, Hongsing P, Chantaravisoot N, Saethang T, Luk-In
658 S, Liao T*et al* (2021). Novel colistin-EDTA combination for successful eradication of colistin-resistant
659 *Klebsiella pneumoniae* catheter-related biofilm infections. *Sci Rep* 11: 21676.
660 Visentin M, Gai Z, Torozi A, Hiller C and Kullak-Ublick GA (2017) Colistin is substrate of the
661 carnitine/organic cation transporter 2 (OCTN2, SLC22A5). *Drug Metab Dispos* 45: 1240-1244.
662 Wang J, Sheng Z, Liu Y, Chen X, Wang S and Yang H (2023) Combined proteomic and transcriptomic
663 analysis of the antimicrobial mechanism of tannic acid against *Staphylococcus aureus*. *Front Pharmacol*
664 14: 1178177.
665 Wayne, PA (2021) Clinical and Laboratory Standards Institute. Performance standards for antimicrobial
666 susceptibility testing: 31st ed. CLSI Supplement M100.
667 Wei P, Song G, Shi M, Zhou Y, Liu Y, Lei J, Chen P and Yin L (2018) Substrate analog interaction with
668 MCR-1 offers insight into the rising threat of the plasmid-mediated transferable colistin resistance. *Faseb j*
669 32: 1085-1098.

670 Wei S, Yang Y, Tian W, Liu M, Yin S and Li J (2020) Synergistic activity of fluoroquinolones combining with
671 artesunate against multidrug-resistant *Escherichia coli*. *Microb Drug Resist* 26: 81-88.
672 Wu C, Liu J, Pan X, Xian W, Li B, Peng W, Wang J, Yang D and Zhou H (2013) Design, synthesis and
673 evaluation of the antibacterial enhancement activities of amino dihydroartemisinin derivatives. *Molecules*
674 18: 6866-6882.
675 Yeh V, Goode A, Johnson D, Cowieson N and Bonev BB (2022) The role of lipid chains as determinants of
676 membrane stability in the presence of styrene. *Langmuir* 38: 1348-1359.
677 Yi K, Liu S, Liu P, Luo X, Zhao J, Yan F, Pan Y, Liu J, Zhai Y, Hu G (2022) Synergistic antibacterial activity
678 of tetrandrine combined with colistin against MCR-mediated colistin-resistant *Salmonella*. Biomed
679 Pharmacother 149: 112873.
680 Zhou Y, Liu B, Chu X, Su J, Xu L, Li L, Deng X and Li D (2022) Commercialized artemisinin derivatives
681 combined with colistin protect against critical Gram-negative bacterial infection. *Commun Biol* 5: 931.
682
683
684
685
686
687
688
689
690

691 **Tables**

692 **Table 1. The antibacterial activities of COL against the tested strains after single and triple**

693 **combinations**

Strains	*mcr-1*	MICs (mg/L)									**Fold change**
		COL alone	COL + 1/4 AS +EDTA				COL + 1/8 AS +EDTA				
			1/4 EDTA	1/8 EDTA	1/16 EDTA	1/32 EDTA	1/4 EDTA	1/8 EDTA	1/16 EDTA	1/23 EDTA	
JS	—	0.25	0.015	0.125	0.125	0.125	0.03	0.25	0.25	0.25	**0-17**
S34	—	0.125	0.008	0.015	0.015	0.015	0.02	0.0625	0.125	0.125	**0-16**
S16	—	4	0.015	0.03	0.0625	0.0625	0.0625	0.125	0.125	0.5	**8-267**
S20	—	2	0.0625	0.125	0.125	0.125	0.25	0.5	0.5	0.5	**4-32**
S13	+	2	0.015	0.125	0.25	0.25	0.0625	0.25	0.5	0.5	**4-133**
S30	+	4	0.015	0.0625	0.0625	0.125	0.125	0.125	0.25	0.5	**8-266.6**
E16	+	2	0.00003	0.002	0.25	0.5	0.004	0.015	0.25	1	**2-66667**
M15	—	＞64	32	32	＞64	＞64	32	32	＞64	＞64	**0-2**
P01	—	＞64	＞64	＞64	＞64	＞64	＞64	＞64	＞64	＞64	**0**

694 Note: COL: colistin; AS: artesunate

695

696

697

698

699

700

701

Figure Legends

Figure 1. Time-kill curves of *Salmonella* strains JS, S16, and S30 with COL alone and in combinations.

a-f Samples were treated with different concentration of COL (0.1 or 2 mg/L), alone or in drug combinations, for 12 h. When used in combination, 1/8 MIC of AS or EDTA was added to a final concentration of 156.3 or 15.6 mg/L, respectively. Counts of CFU/mL were performed on all cultures at each time point, and data are mean ± SD from representative of three independent experiments. CON indicates the negative control group.

Figure 2. AS, EDTA, and COL affected membrane integrity, PMF, ROS, and H_2O_2 levels in S16 and S30 strains..

Different concentration of COL (0.1 or 2 mg/L) were used alone or in combination with AS and EDTA. When used in combination, 1/8 MIC of AS or EDTA was added to a final concentration of 156.3 or 15.6 mg/L, respectively.

a-d AS, EDTA, and COL affected membrane integrity as measured by fluorescence probes NPN and PI. Error bars indicated standard deviations for 3 replicas (* $p < 0.001$, ns not significant). CON indicates the negative control group, and SOV indicates the solvent-exposed group.

e-h Disruption of PMF is shown by measuring the dissipation of electric potential ($\Delta\psi$) (a, b) and osmotic component (ΔpH) (c, d). Error bars indicate standard deviations for 3 replicas (* $p < 0.001$, ns not significant). CON indicates the negative control group, and SOV indicates the solvent-exposed group.

i-l Intracellular accumulation of ROS (i, j) and H_2O_2 (k, l) in S16 and S30 strains after 1 h treatment. Data were shown in the mean of triplicates ± SD (* $p < 0.001$, ns not significant). CON indicates the

723 negative control group, SOV indicates the solvent-exposed group, and POS indicates the positive
724 control group that treated with Rosup from the Total ROS Detection Kit.
725
726 **Figure 3. Morphological changes of S16 (*mcr-1*$^-$) strain.**
727 The images were obtained after the treatment with COL (2 mg/L) alone or in combination with 1/8 MIC of AS
728 (156.3 mg/L) or EDTA (15.6 mg/L). CON indicates the negative control group, and SOV indicates the
729 solvent-exposed group. Red arrows indicate the cell damages characterized by folds, crevices, or depressions.
730
731 **Figure 4. KEGG pathway analysis of SDEGs in S16 (a, b, c) and S30 (d, e, f) strains within the AEC .vs.**
732 **C, AEC .vs. AC, and AEC .vs. EC groups.**
733 Samples were harvested after the trestment of COL (2 mg/L) alone or in combination with 1/8 MIC of
734 AS (156.3 mg/L) or EDTA (15.6 mg/L) for 6 h. Pathway name and number of down-regulated (blue),
735 up-regulated (red) genes in each pathway are indicated in parentheses on the left (down/up).
736 Highlighted with red circles are the pathways that SDEGs mainly enriched and appeared
737 simultaneously in different comparison groups.
738
739 **Figure 5. The SDEGs detected in two component system (a, b), flagellar assembly (c, d) and ABC**
740 **transporters (e, f) pathways among different comparison groups, within S16 and S30 strains.**
741 Samples were harvested after the treatment of COL (2 mg/L) alone or in combination with 1/8 MIC of
742 AS (156.3 mg/L) or EDTA (15.6 mg/L) for 6 h. Labels in each square indicate the $\log_2$ (fold change) of
743 corresponding genes. Squares without label and gray background indicate the data are not credible (p >

744 0.05, |log_2Fold Change| < 1.0). Background colors indicate the expression levels of the respective genes,

745 red = up-regulated, blue = down-regulated. log_2FC: log_2Fold Change.

746

747 **Figure 6. The SDMs detected in archidonic acid metabolism, degradation of aromatic compounds ,**

748 **taurine and hypotaurine metabolism pathways among different comparison groups, within S16 (a) and**

749 **S30 (b) strains.**

750 Samples were harvested after the treatment of COL (2 mg/L) alone or in combination with 1/8 MIC of

751 AS (156.3 mg/L) or EDTA (15.6 mg/L) for 6 h. Labels in each square indicate the fold changes of

752 corresponding metabolites. Squares without label and gray background indicate the data are not

753 credible (VIP < 1.0, 0.833 > Fold Change < 1.2 or Fold Change $\leq$ 0.833, $p \geq 0.05$). Background

754 colors indicate the fold changes of the respective metabolites, red = increased, blue = decreased.

755

756 **Figure 7. AS and EDTA potentiate colistin activity against *Salmonella* S30 (*mcr-1*$^+$) *in vivo*.**

757 Kunming mice (n=6 per group) were intraperitoneally given a non-lethal dose of *Salmonella* S30 (1.31

758 $\times$ 10^5 CFU), then treated with PBS, COL (10 mg/kg), AS (15 mg/kg), AS (15 mg/kg) + COL (10

759 mg/kg), EDTA (50 mg/kg) + COL (10 mg/kg), and AS (15 mg/kg) + EDTA (50 mg/kg)+ COL (10

760 mg/kg) by intraperitoneal injection. Bacterial loads were determined in spleen and liver and bacterial

761 counts were computed and presented as the mean $\pm$ SD log_{10} CFU/mL. The p values were determined

762 by one-way ANOVA (* $p < 0.001$, ns not significant).

763

764 **Figure 8. Scheme summarizing the proposed mechanisms that AS and EDTA enhancing the**

765 **antibacterial effect of COL against *Salmonella*.**

766 ① COL and EDTA cause the membrane damages by targeting LPS and chelating cations, which punch
767 holes in both the outer membrane (OM) and inner membrane (IM). ② AEC combination collapses the
768 Δψ component of Proton Motive Force (PMF) in *Salmonella.* ③ The down-regulated lipid compounds
769 prostaglandins (PGs) lead to perturbtion of membrane phospholipids in cell membranes. ④
770 Accumulation of toxic compounds (eg. styrene, ROS *et al*) could accelerate the destruction of cell
771 membrane. ⑤ The down-regulation of chemotaxis, flagellar assembly, *Salmonella* infection related
772 genes indicate impaired virulence of *Salmonella.* ⑥ The down-regulation of genes in ABC transporters
773 indicate impaired stress tolerance of *Salmonella*. ⑦ AEC treatment results in the down-rugulation of
774 flagellar assembly related genes and defective of flagellum. ⑧ AS was capable of significantly
775 enhancing the antibacterial activities of antibiotics against *E. coli,* via inhibition of the efflux pumps. ⑨
776 AS could be developed as the a MCR-1 inhibitor, which may work synergistically with the EDTA
777 chelation to inhibit MCR-1 and contribute to reverse the COL resistance of *mcr-1*-harboring *Salmonella*
778 strains. FC: Fold Change.

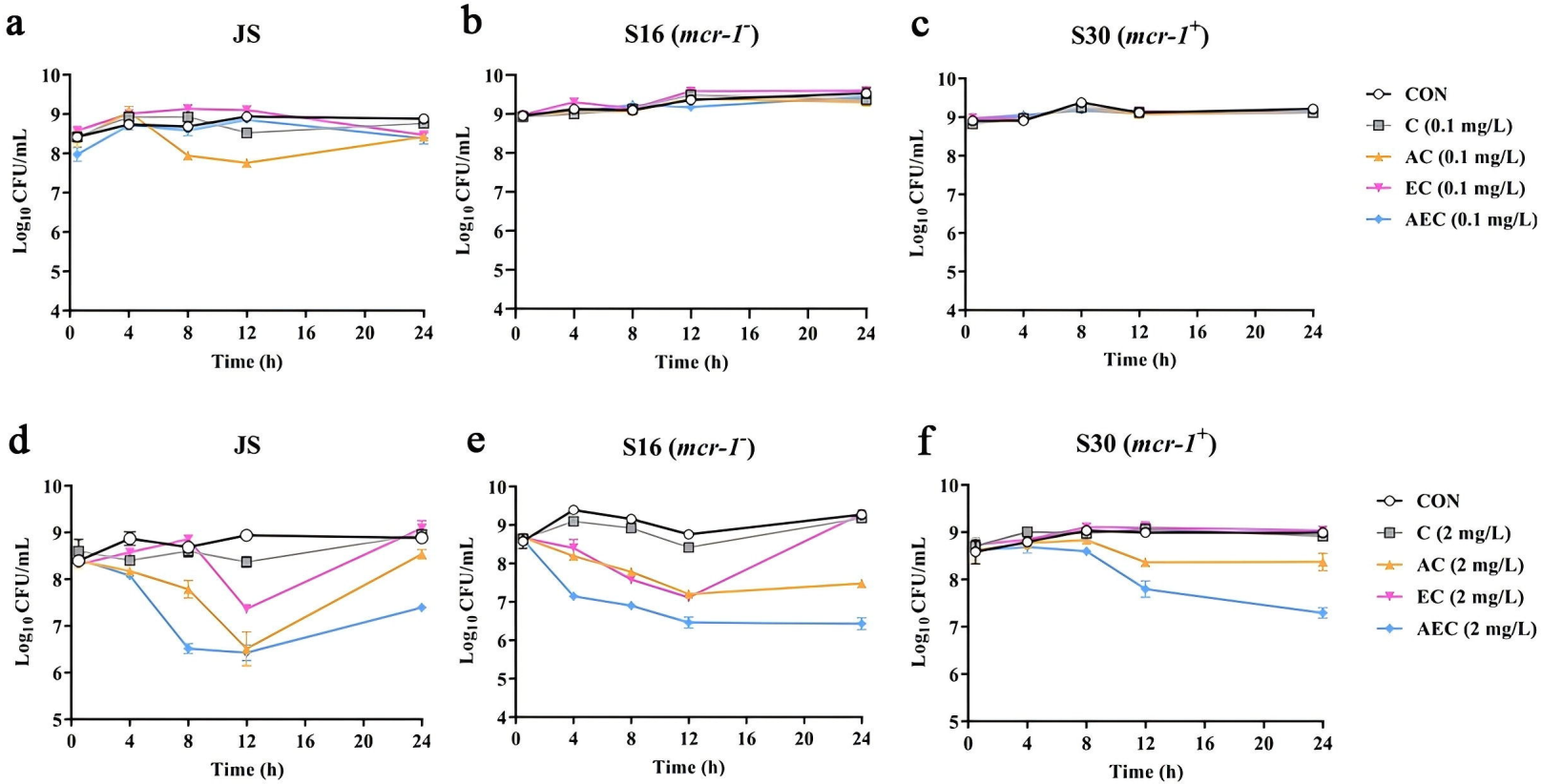
a
JS
b
S16 (mcr-1⁻)
c
S30 (mcr-1⁺)
d
JS
e
S16 (mcr-1⁻)
f
S30 (mcr-1⁺)
Log10 CFU/mL
Time (h)
CON
C (0.1 mg/L)
AC (0.1 mg/L)
EC (0.1 mg/L)
AEC (0.1 mg/L)
C (2 mg/L)
AC (2 mg/L)
EC (2 mg/L)
AEC (2 mg/L)

Outer membrane

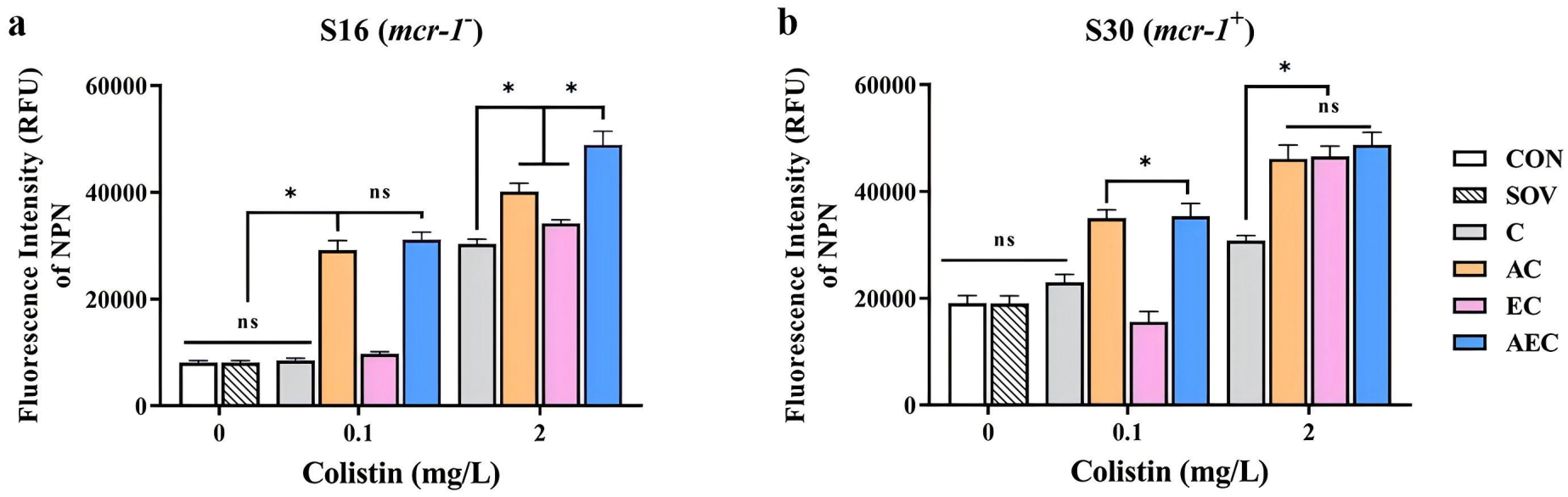

Inner permeability

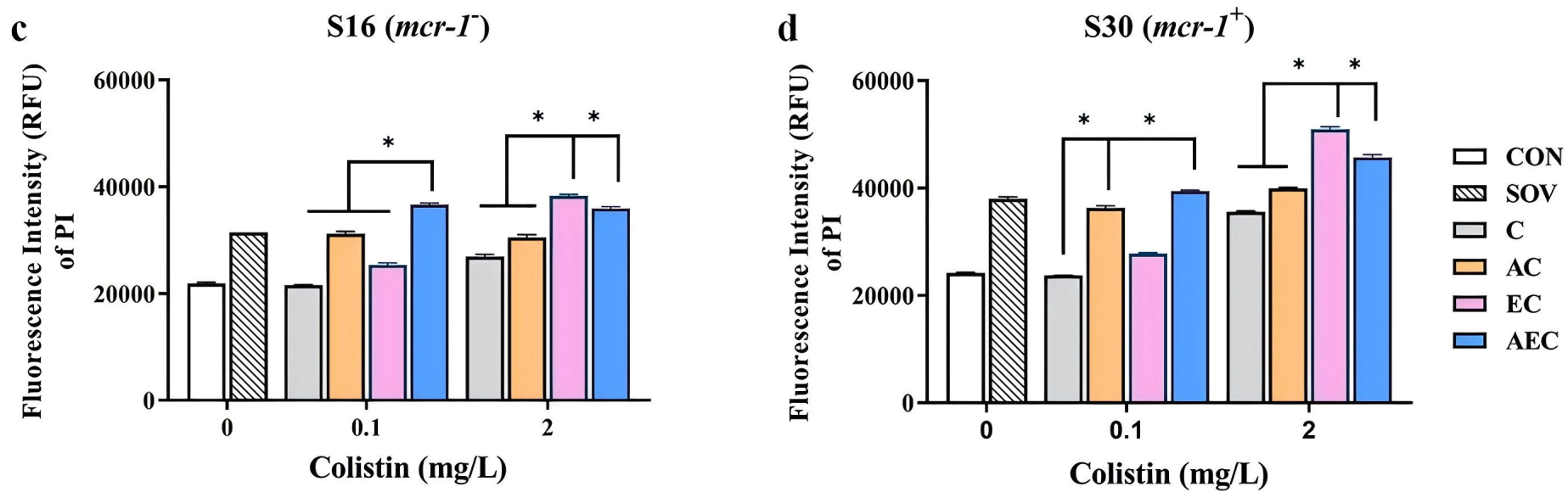

ΔΨ

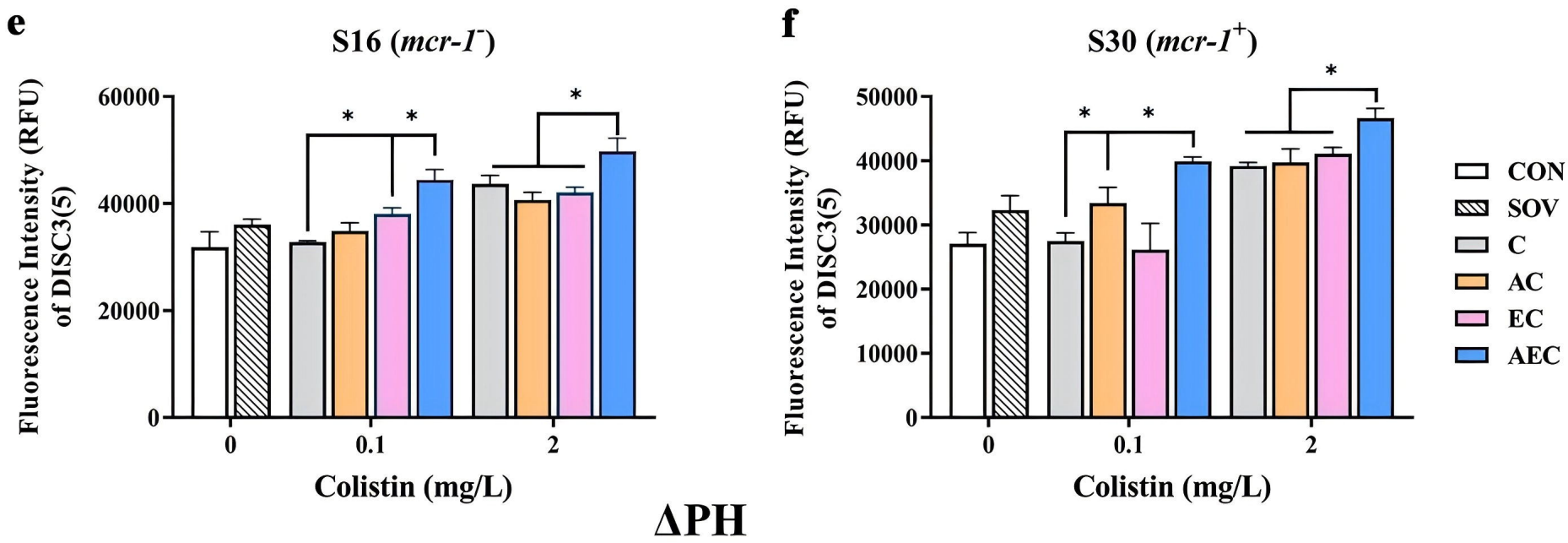

ΔPH

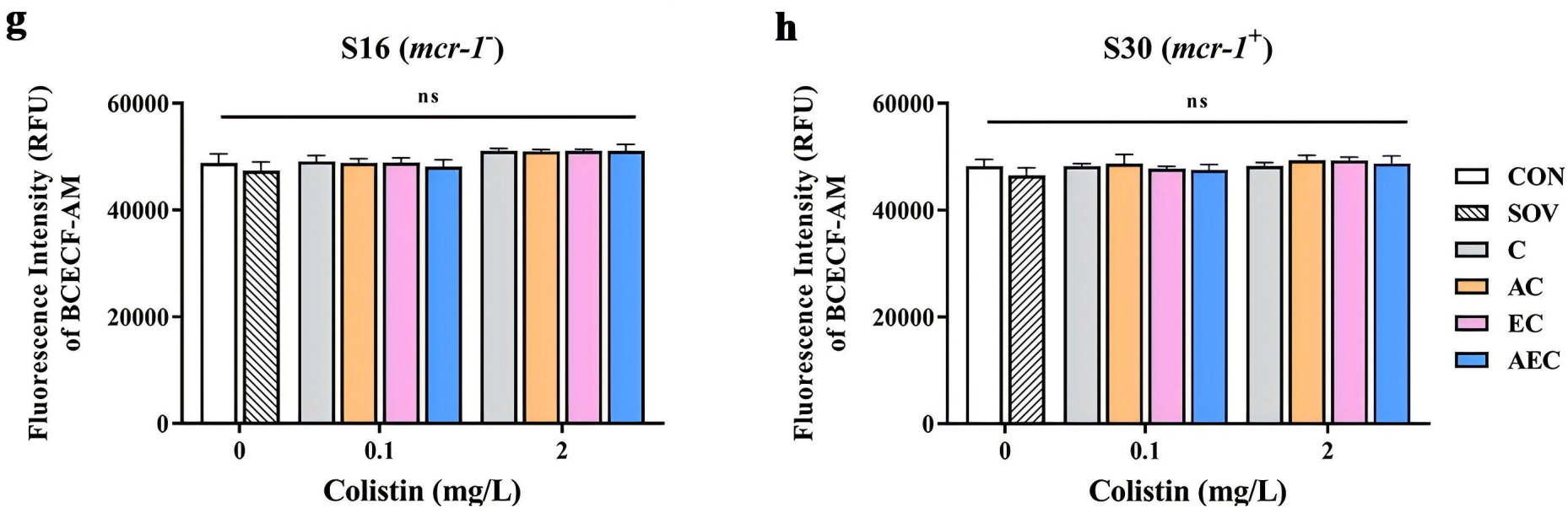

ROS

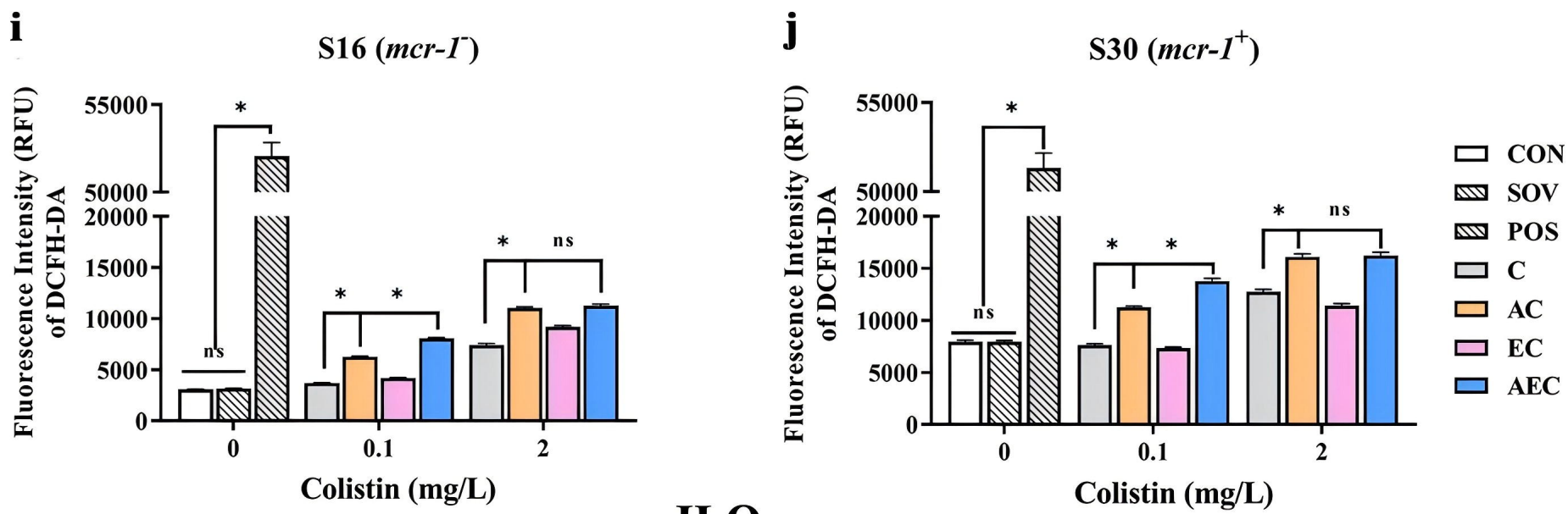

H_2O_2

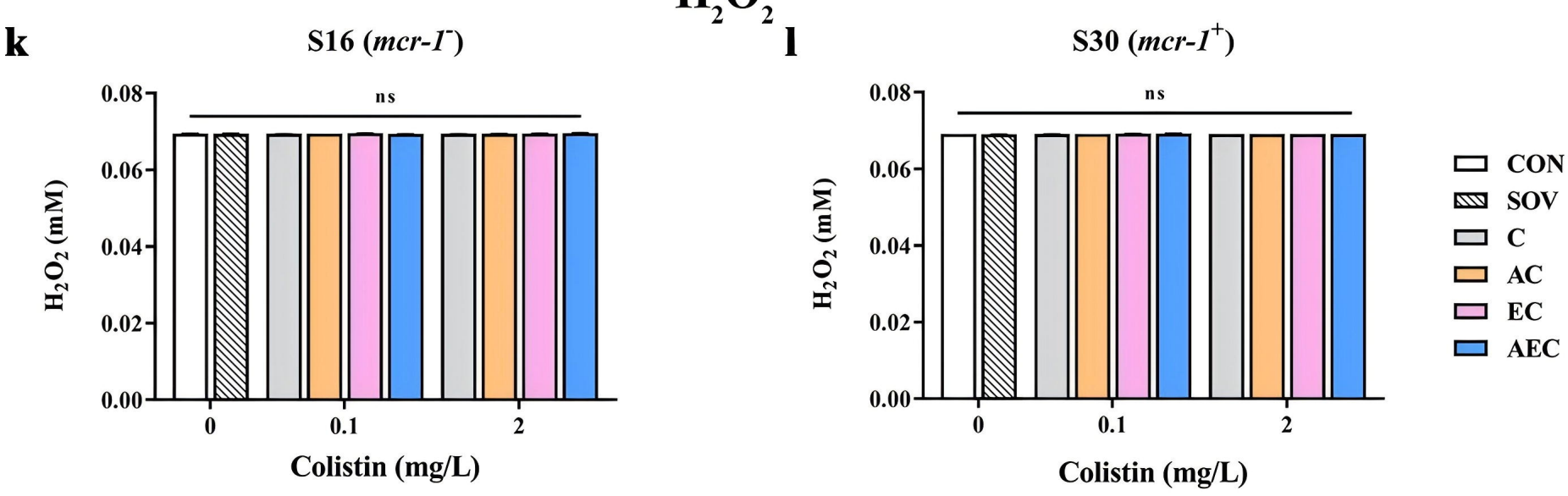

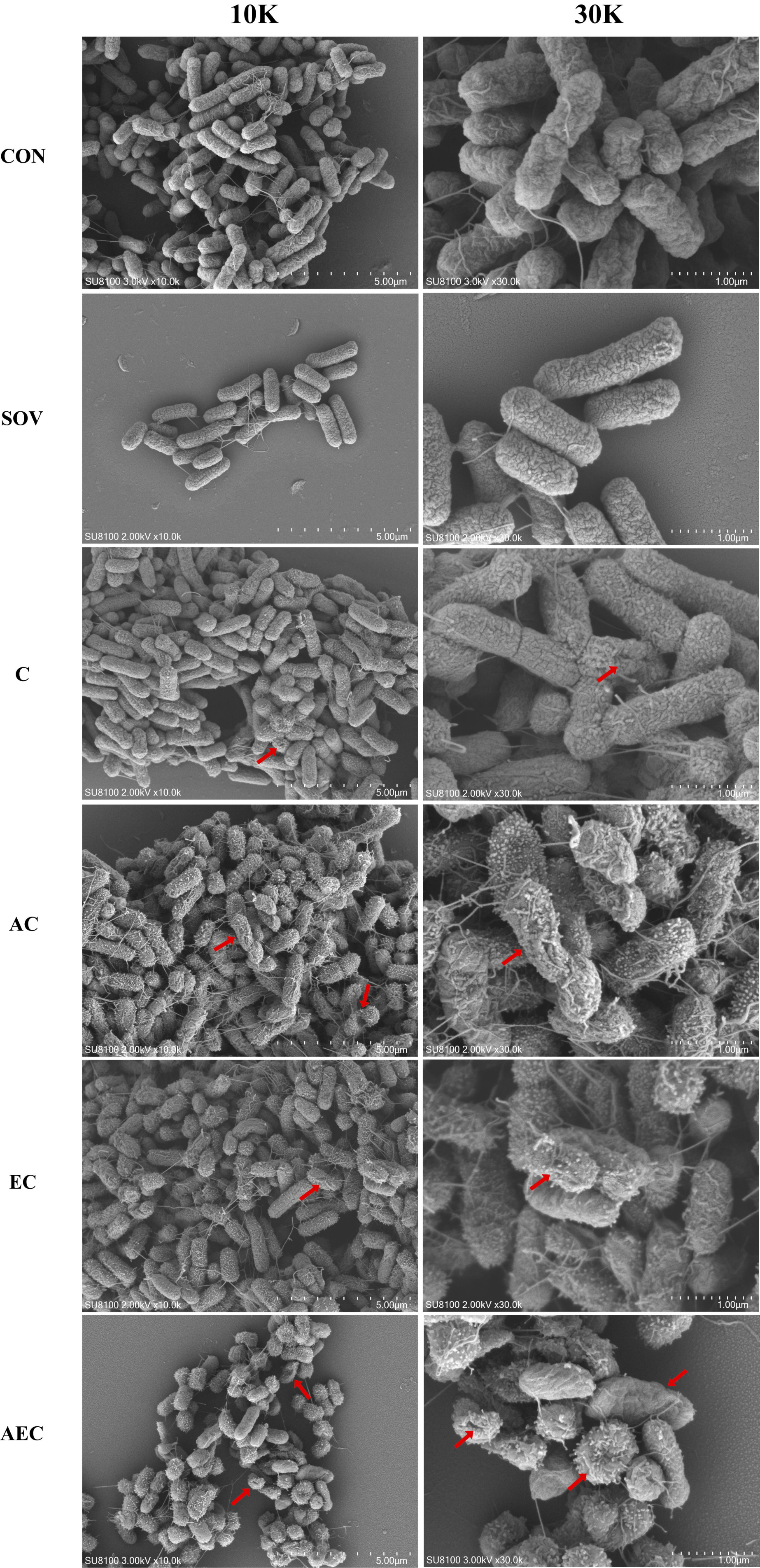
10K
30K
CON
SOV
C
AC
EC
AEC
SU8100 3.0kV x10.0k
5.00µm
SU8100 3.0kV x30.0k
1.00µm
SU8100 2.00kV x10.0k
5.00µm
SU8100 2.00kV x30.0k
1.00µm
SU8100 2.00kV x10.0k
5.00µm
SU8100 2.00kV x30.0k
1.00µm
SU8100 2.00kV x10.0k
5.00µm
SU8100 2.00kV x30.0k
1.00µm
SU8100 2.00kV x10.0k
5.00µm
SU8100 2.00kV x30.0k
1.00µm
SU8100 3.00kV x10.0k
5.00µm
SU8100 3.00kV x30.0k
1.00µm

S16 (*mcr-1*$^{-}$)

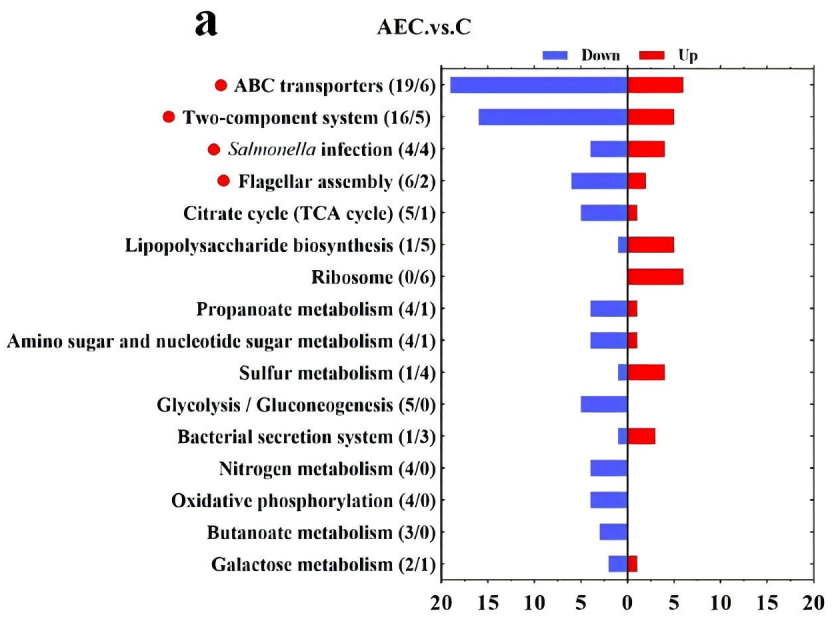

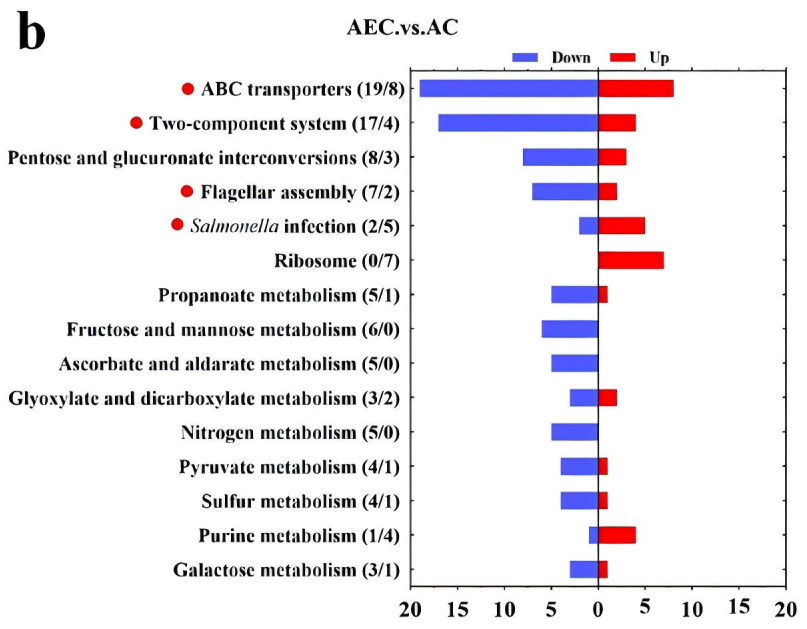

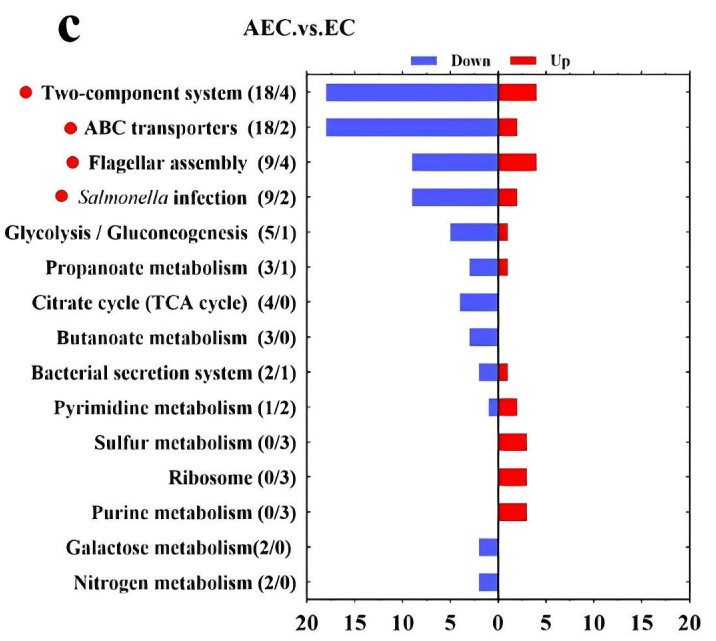

S30 (*mcr-1*$^{+}$)

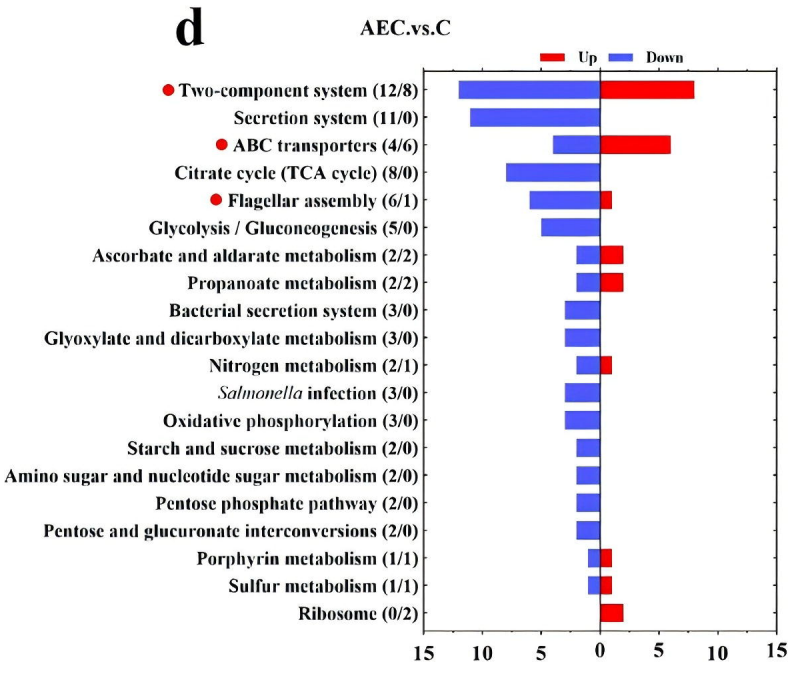

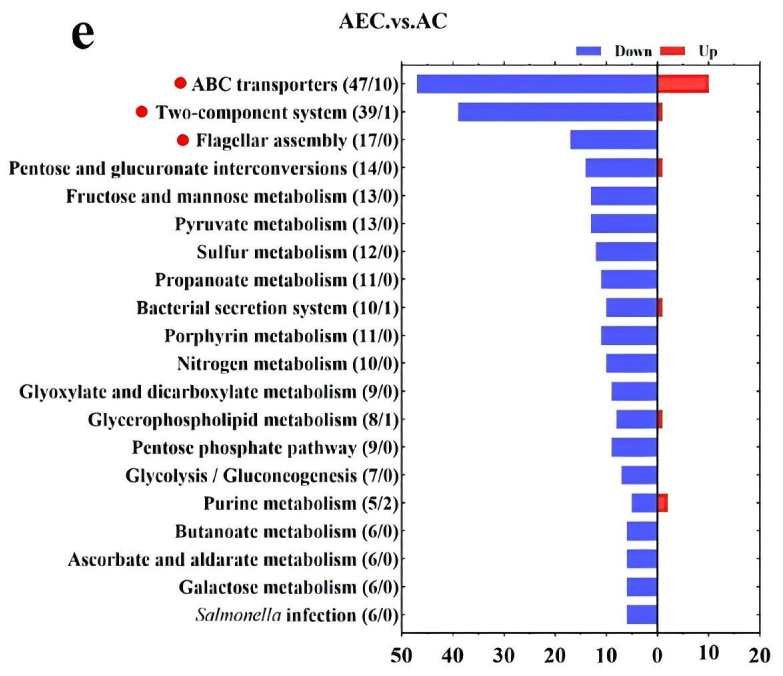

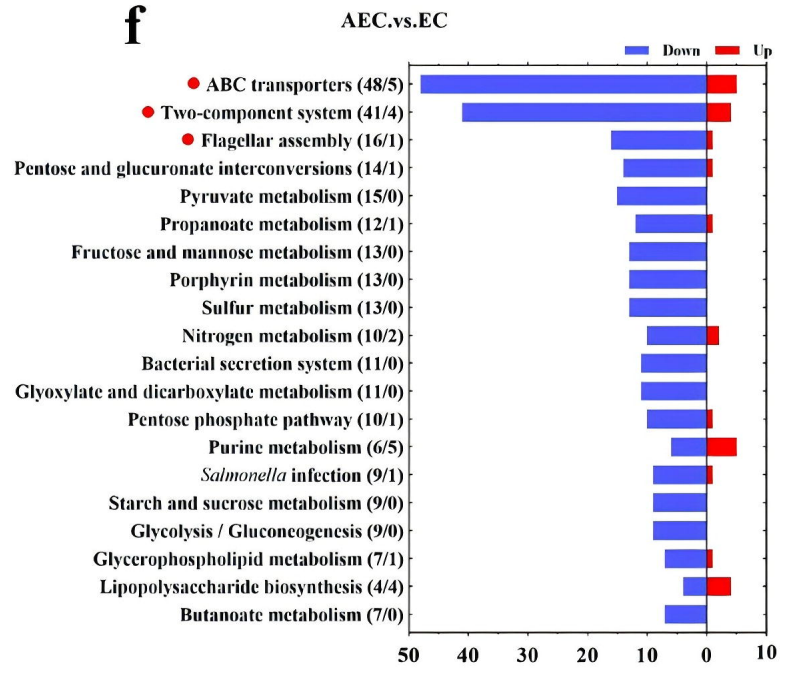

Two-component system

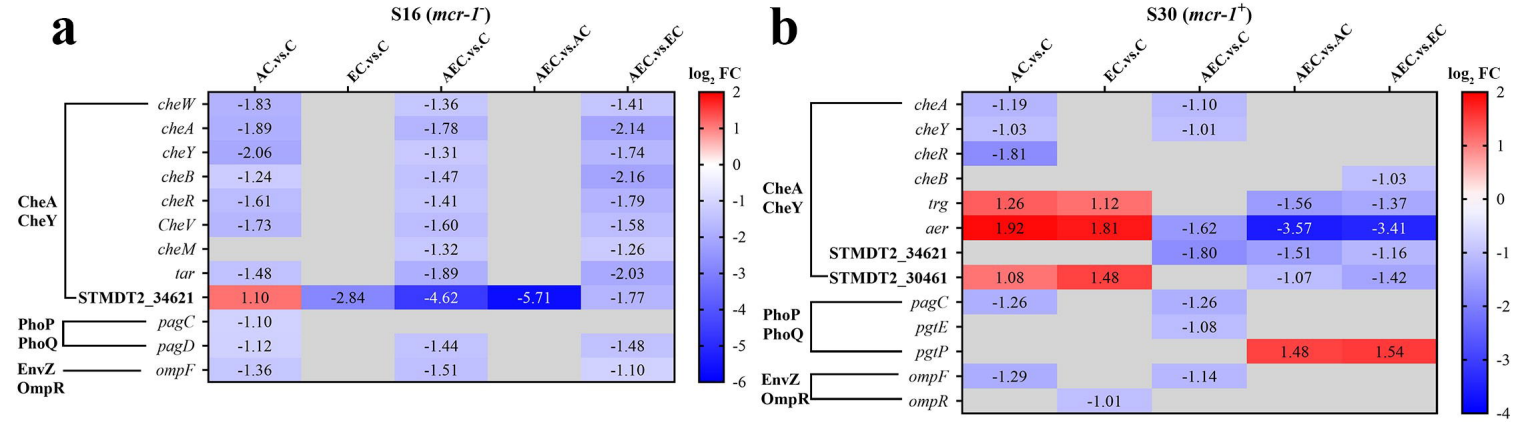

Flagellar assembly

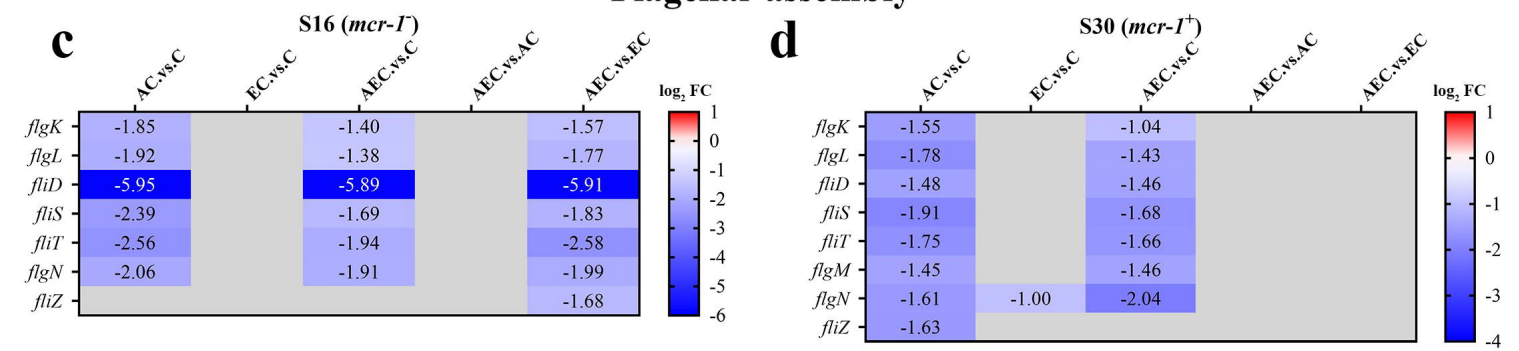

ABC transporters

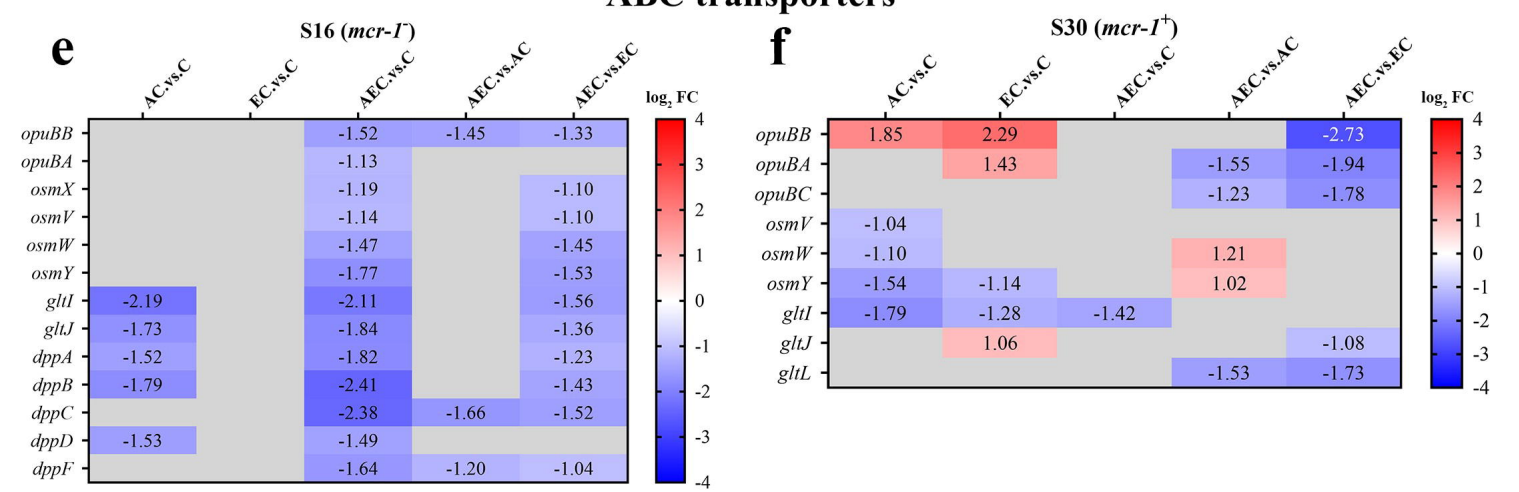

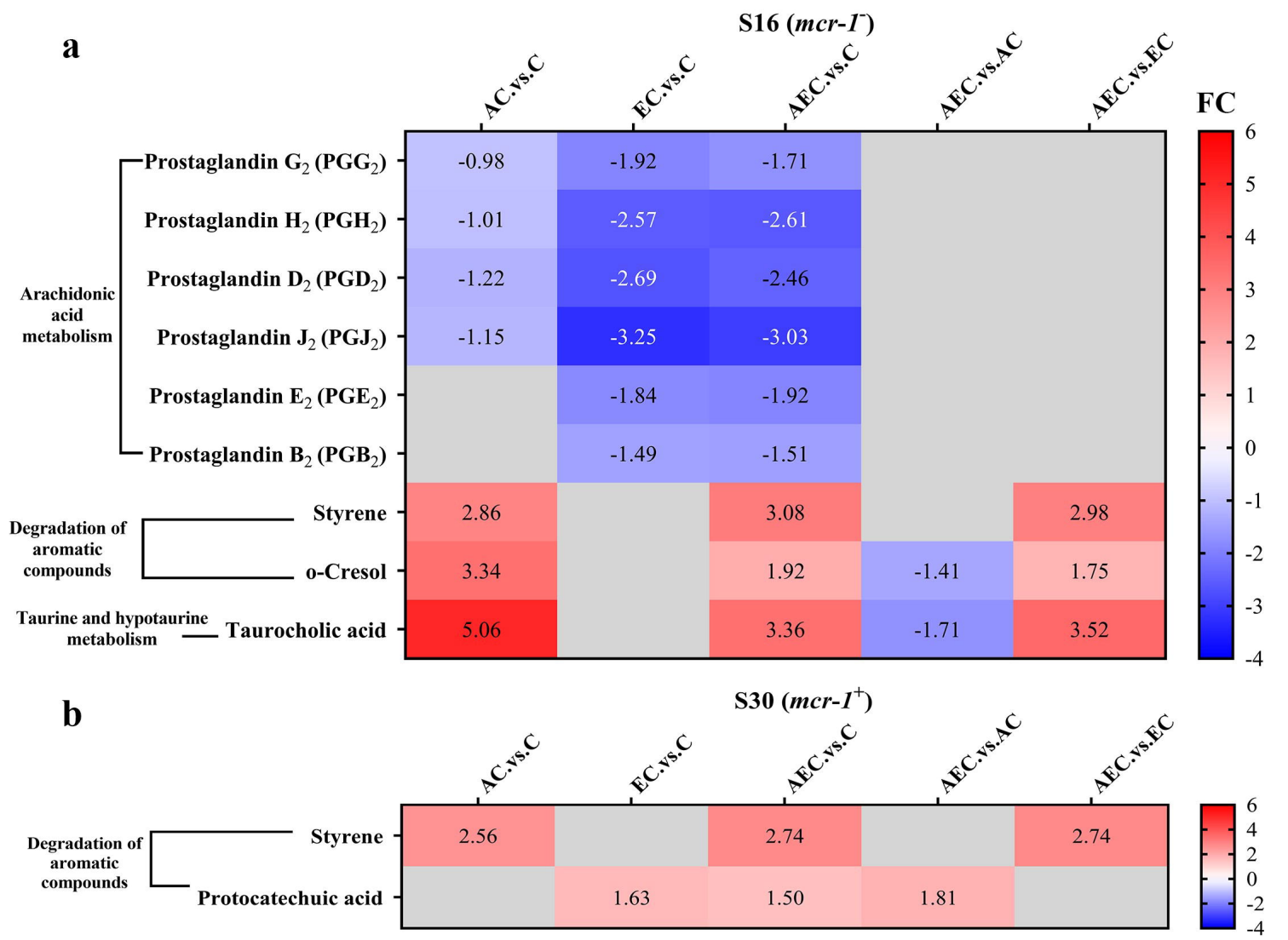
a
S16 (mcr-1⁻)
AC.vs.C
EC.vs.C
AEC.vs.C
AEC.vs.AC
AEC.vs.EC
FC
Arachidonic acid metabolism
Prostaglandin G2 (PGG2)
Prostaglandin H2 (PGH2)
Prostaglandin D2 (PGD2)
Prostaglandin J2 (PGJ2)
Prostaglandin E2 (PGE2)
Prostaglandin B2 (PGB2)
Degradation of aromatic compounds
Styrene
o-Cresol
Taurine and hypotaurine metabolism
Taurocholic acid
-0.98
-1.92
-1.71
-1.01
-2.57
-2.61
-1.22
-2.69
-2.46
-1.15
-3.25
-3.03
-1.84
-1.92
-1.49
-1.51
2.86
3.08
2.98
3.34
1.92
-1.41
1.75
5.06
3.36
-1.71
3.52
6
5
4
3
2
1
0
-1
-2
-3
-4
b
S30 (mcr-1⁺)
AC.vs.C
EC.vs.C
AEC.vs.C
AEC.vs.AC
AEC.vs.EC
Degradation of aromatic compounds
Styrene
Protocatechuic acid
2.56
2.74
2.74
1.63
1.50
1.81
6
4
2
0
-2
-4

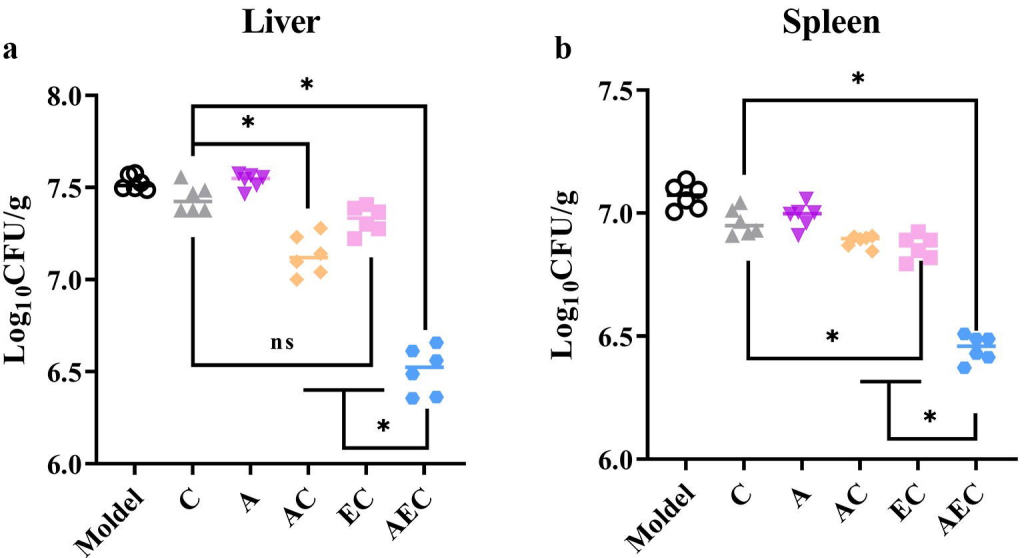
a
Liver
8.0
7.5
7.0
6.5
6.0
Log10CFU/g
*
*
ns
*
Moldel
C
A
AC
EC
AEC
b
Spleen
7.5
7.0
6.5
6.0
Log10CFU/g
*
*
*
Moldel
C
A
AC
EC
AEC

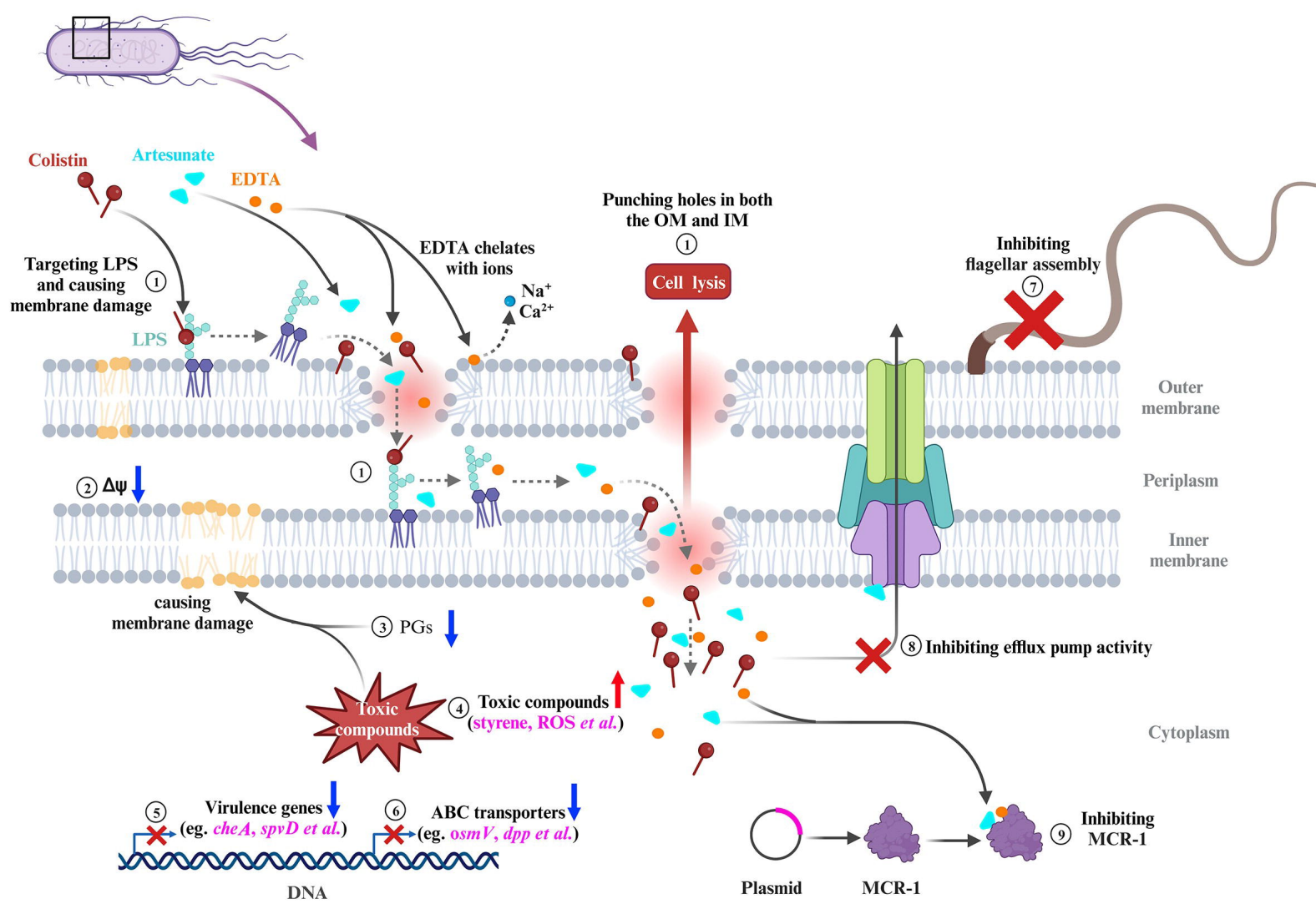
Colistin
Artesunate
EDTA
Targeting LPS and causing membrane damage
1
LPS
EDTA chelates with ions
Na+
Ca2+
Punching holes in both the OM and IM
1
Cell lysis
Inhibiting flagellar assembly
7
Outer membrane
Periplasm
Inner membrane
2 Δψ
1
causing membrane damage
3 PGs
Toxic compounds
4 Toxic compounds
(styrene, ROS et al.)
8 Inhibiting efflux pump activity
Cytoplasm
5 Virulence genes
(eg. cheA, spvD et al.)
6 ABC transporters
(eg. osmV, dpp et al.)
DNA
Plasmid
MCR-1
9 Inhibiting MCR-1

ROS

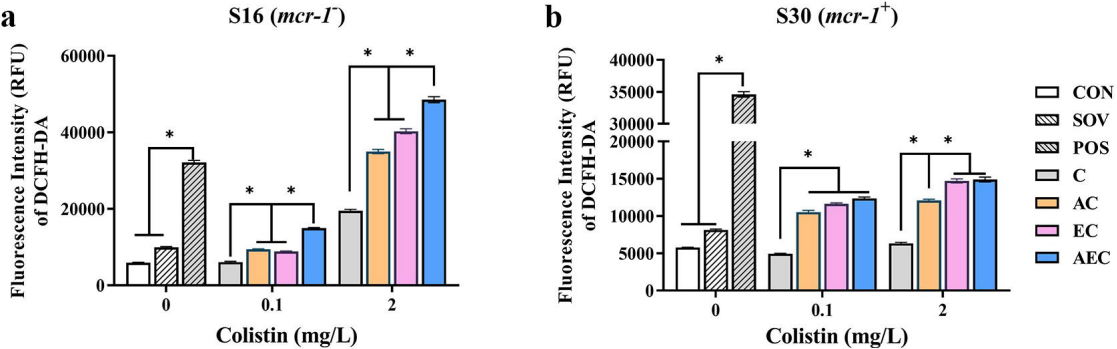
a
S16 (mcr-1⁻)
Fluorescence Intensity (RFU) of DCFH-DA
60000
40000
20000
0
0
0.1
2
Colistin (mg/L)
b
S30 (mcr-1⁺)
Fluorescence Intensity (RFU) of DCFH-DA
40000
35000
30000
20000
15000
10000
5000
0
0
0.1
2
Colistin (mg/L)
CON
SOV
POS
C
AC
EC
AEC

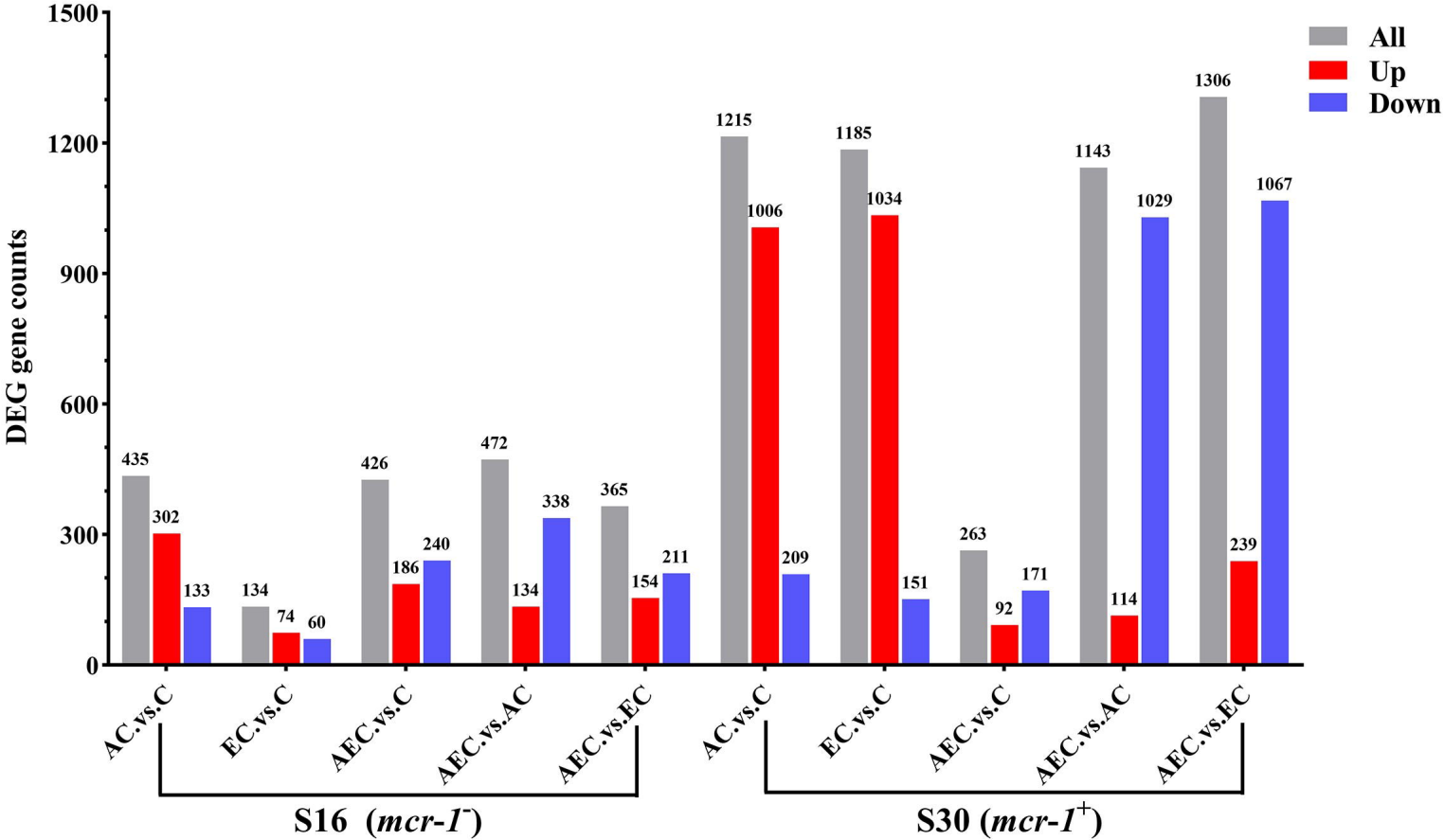
DEG gene counts
1500
1200
900
600
300
0
All
Up
Down
435
302
133
134
74
60
426
186
240
472
134
338
365
154
211
1215
1006
209
1185
1034
151
263
92
171
1143
114
1029
1306
239
1067
AC.vs.C
EC.vs.C
AEC.vs.C
AEC.vs.AC
AEC.vs.EC
AC.vs.C
EC.vs.C
AEC.vs.C
AEC.vs.AC
AEC.vs.EC
S16 (mcr-1⁻)
S30 (mcr-1⁺)

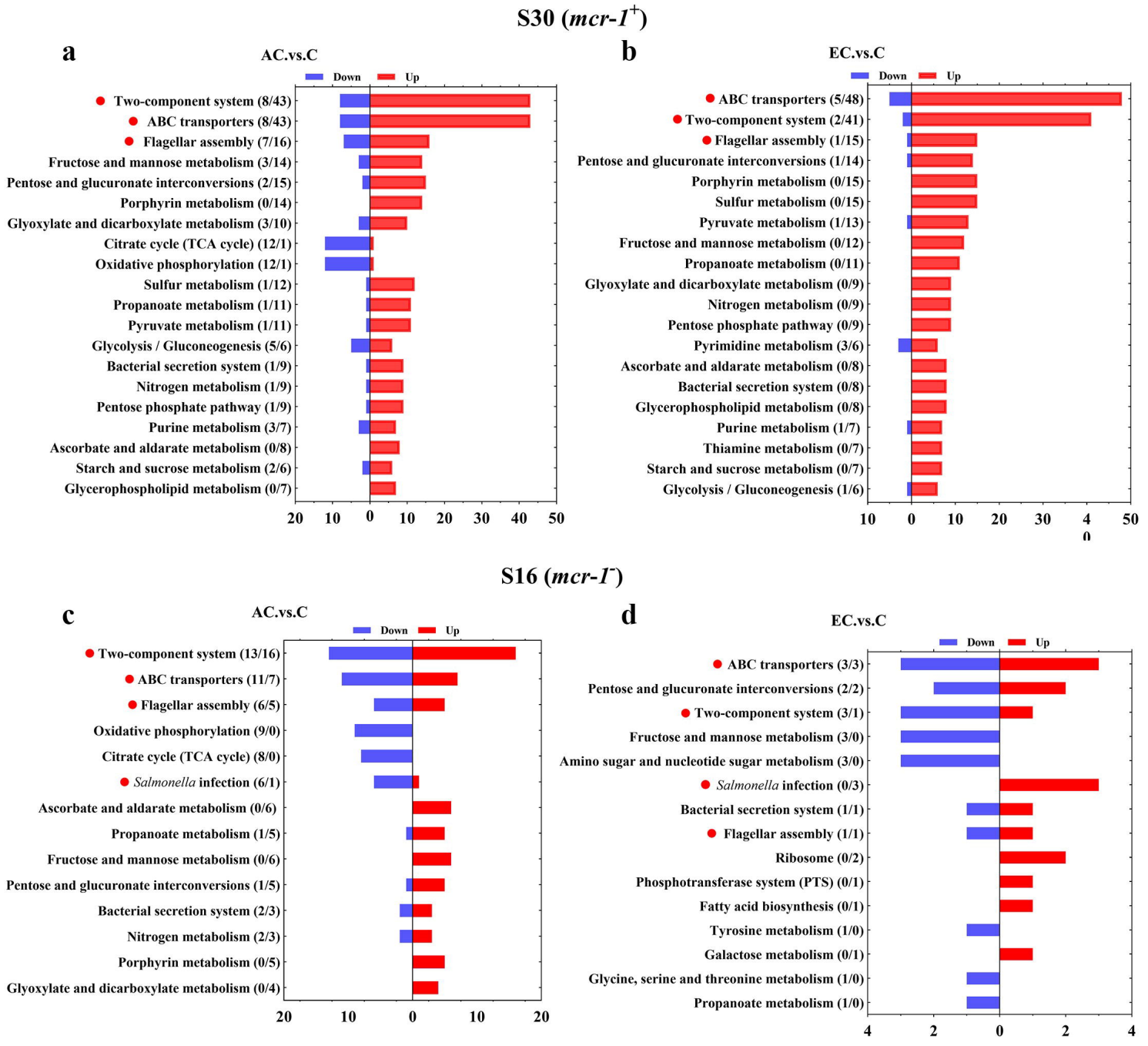
S30 (mcr-1+)
a
AC.vs.C
Down
Up
Two-component system (8/43)
ABC transporters (8/43)
Flagellar assembly (7/16)
Fructose and mannose metabolism (3/14)
Pentose and glucuronate interconversions (2/15)
Porphyrin metabolism (0/14)
Glyoxylate and dicarboxylate metabolism (3/10)
Citrate cycle (TCA cycle) (12/1)
Oxidative phosphorylation (12/1)
Sulfur metabolism (1/12)
Propanoate metabolism (1/11)
Pyruvate metabolism (1/11)
Glycolysis / Gluconeogenesis (5/6)
Bacterial secretion system (1/9)
Nitrogen metabolism (1/9)
Pentose phosphate pathway (1/9)
Purine metabolism (3/7)
Ascorbate and aldarate metabolism (0/8)
Starch and sucrose metabolism (2/6)
Glycerophospholipid metabolism (0/7)
20 10 0 10 20 30 40 50
b
EC.vs.C
Down
Up
ABC transporters (5/48)
Two-component system (2/41)
Flagellar assembly (1/15)
Pentose and glucuronate interconversions (1/14)
Porphyrin metabolism (0/15)
Sulfur metabolism (0/15)
Pyruvate metabolism (1/13)
Fructose and mannose metabolism (0/12)
Propanoate metabolism (0/11)
Glyoxylate and dicarboxylate metabolism (0/9)
Nitrogen metabolism (0/9)
Pentose phosphate pathway (0/9)
Pyrimidine metabolism (3/6)
Ascorbate and aldarate metabolism (0/8)
Bacterial secretion system (0/8)
Glycerophospholipid metabolism (0/8)
Purine metabolism (1/7)
Thiamine metabolism (0/7)
Starch and sucrose metabolism (0/7)
Glycolysis / Gluconeogenesis (1/6)
10 0 10 20 30 4 50
0
S16 (mcr-1-)
c
AC.vs.C
Down
Up
Two-component system (13/16)
ABC transporters (11/7)
Flagellar assembly (6/5)
Oxidative phosphorylation (9/0)
Citrate cycle (TCA cycle) (8/0)
Salmonella infection (6/1)
Ascorbate and aldarate metabolism (0/6)
Propanoate metabolism (1/5)
Fructose and mannose metabolism (0/6)
Pentose and glucuronate interconversions (1/5)
Bacterial secretion system (2/3)
Nitrogen metabolism (2/3)
Porphyrin metabolism (0/5)
Glyoxylate and dicarboxylate metabolism (0/4)
20 10 0 10 20
d
EC.vs.C
Down
Up
ABC transporters (3/3)
Pentose and glucuronate interconversions (2/2)
Two-component system (3/1)
Fructose and mannose metabolism (3/0)
Amino sugar and nucleotide sugar metabolism (3/0)
Salmonella infection (0/3)
Bacterial secretion system (1/1)
Flagellar assembly (1/1)
Ribosome (0/2)
Phosphotransferase system (PTS) (0/1)
Fatty acid biosynthesis (0/1)
Tyrosine metabolism (1/0)
Galactose metabolism (0/1)
Glycine, serine and threonine metabolism (1/0)
Propanoate metabolism (1/0)
4 2 0 2 4

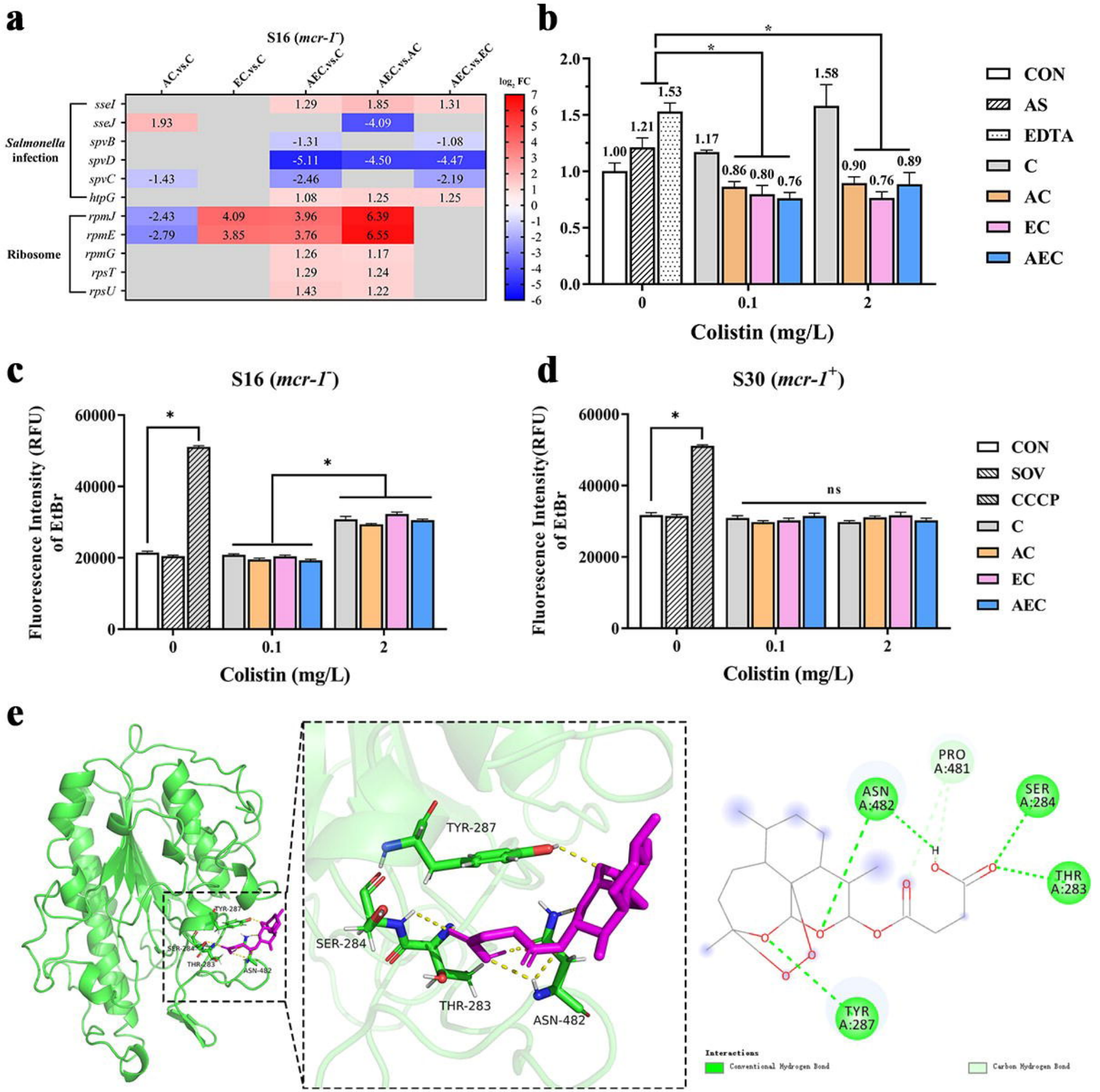
a
S16 (mcr-1⁻)
AC.vs.C
EC.vs.C
AEC.vs.C
AEC.vs.AC
AEC.vs.EC
Salmonella infection
sseI
sseJ
spvB
spvD
spvC
htpG
Ribosome
rpmJ
rpmE
rpmG
rpsT
rpsU
log2 FC
b
CON
AS
EDTA
C
AC
EC
AEC
Colistin (mg/L)
c
S16 (mcr-1⁻)
Fluorescence Intensity (RFU) of EtBr
Colistin (mg/L)
d
S30 (mcr-1⁺)
Fluorescence Intensity(RFU) of EtBr
CON
SOV
CCCP
C
AC
EC
AEC
ns
Colistin (mg/L)
e
TYR-287
SER-284
THR-283
ASN-482
PRO A:481
ASN A:482
SER A:284
THR A:283
TYR A:287
Interactions
Conventional Hydrogen Bond
Carbon Hydrogen Bond

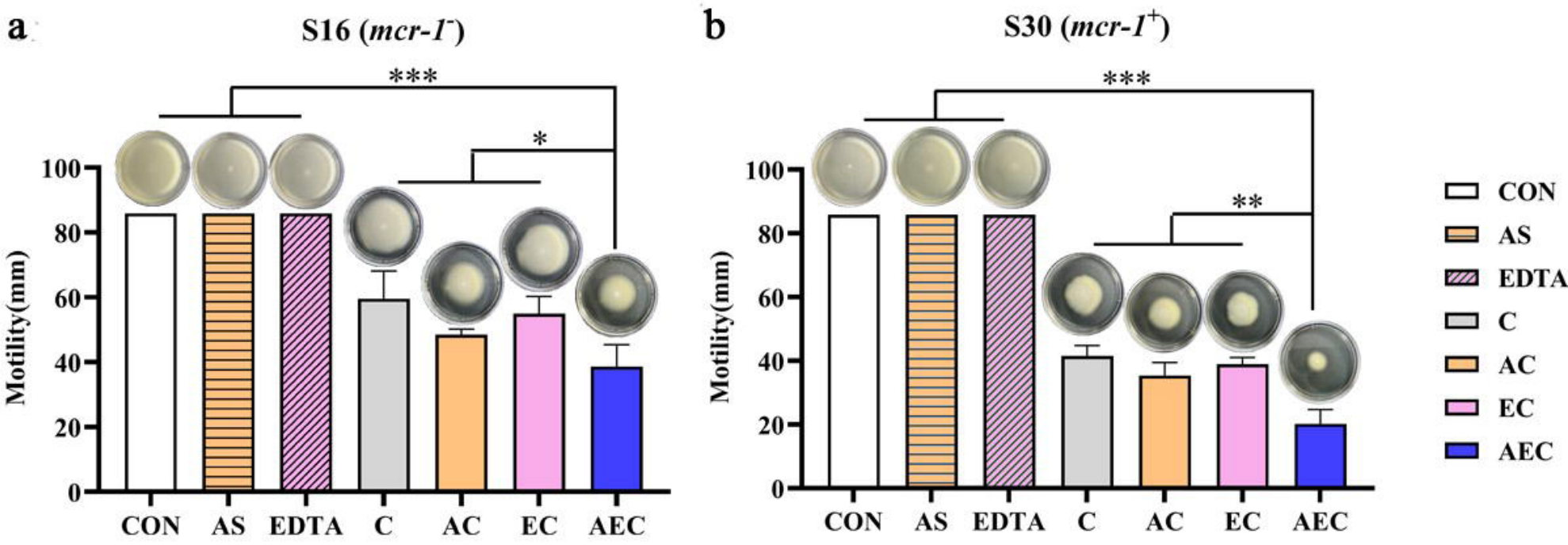
a
S16 (mcr-1⁻)
***
*
Motility(mm)
100
80
60
40
20
0
CON
AS
EDTA
C
AC
EC
AEC
b
S30 (mcr-1⁺)
***
**
Motility(mm)
100
80
60
40
20
0
CON
AS
EDTA
C
AC
EC
AEC
CON
AS
EDTA
C
AC
EC
AEC